CDF/ANAL/QCD/MIN_BIAS/CDFR/10039
01/11/2010

Lambda, Cascade and Omega Production from Minimum Biased Events

Seog Oh[1], Amy Wen[2]
Chiho Wang[3], Thomas Phillips[4]
Jared Yamaoka[5] ,Geumbong Yu[6]

Duke University

Abstract

We present the inclusive invariant p_t cross section of hyperons, lambdas, cascades and omegas in the minimum biased events. The cross section is also divided according to the event multiplicity.

[1] seog@phy.duke.edu
[2] Amy.wen@phy.duke.edu
[3] chiho@phy.duke.edu
[4] phillips@phy.duke.edu
[5] yamaoka@phy.duke.edu
[6] gbyu@fnal.gov

1. Introduction

Since the discovery of Ks and lambdas from cosmic ray interactions in 1947[1], the production properties of hyperons from hadron and hadron collisions have been studied, including at $Sp\bar{p}S$ [2] and the early Tevatron collider[3, 4]. Particles with strangeness have been also a favorite subject in heavy ion collisions, because if QGP (quark-gluon plasma) is formed, one of its signatures is the enhanced production of particles with strangeness. The studies of lambdas and cascades at $Sp\bar{p}S$ and Tevatron were low in statistics and thus limited to less than a few GeV p_t region and there have been no analyses involving omegas. Using CDF Run II data, we report on the invariant inclusive p_t distribution of lambdas, cascades and omegas up to 10 GeV p_t as a function of event multiplicity. The omega sample size is the largest since the discovery of omega [5].

2. Data , MC data and event selection

The data for this analysis is from minimum biased trigger. The data sets are listed in Table 1. There are about 100 million events in the data sets. The events with Z vertex within +/- 60 cm are selected for further processing. An event could have several vertices when the instantaneous luminosity is high. If there is more than one vertex, then the vertex with highest quality is chosen. This vertex is usually the one with the most tracks. Moreover we require that there are no other Z vertices nearby, within +/-5.0 cm of the vertex. This is to insure that the resonances are from the chosen vertex.

There are three types of MC data used in this analysis. The first is the simulation using PYTHIA minimum biased events. This is to compare the general data characteristics with real data. Another type is single resonance MC data and the third one is single resonance mixed with different numbers of minimum biased events. The single resonance MC data is used to develop cuts, and the last one is used to calculate the efficiency of detecting the resonance. In the single resonance MC data, there is only one resonance per event generated with fixed p_t and uniform in pseudo-rapidity between -2 and 2. The mixed MC data are generated by mixing a resonance (at one fixed p_t and uniform in pseudo-rapidity between -2 and 2) with a different number of PYTHIA minimum biased events. These events are input to CDFSIM, and the reconstructed events are processed like the real events. Typically we generate 100,000 events for one p_t point. The p_t values are varied between 0.5 GeV and 10 GeV and there are more than 10 p_t points for one resonance. For the mixed case, two sets of data are generated with different number of minimum biased events mixed in: one set always has one event mixed in, and the other has four events mixed in on average and the actual number of mixed events follows a Poisson distribution. Our default efficiency is the latter and the difference in efficiency between the two is used as one of our systematic errors.

Data Set
gmbsbd, gmbsah, gmbsai, gmbsbi, gmbsbj, gmbsbk, gmbsbm

Table 1. The data sets used in this analysis.

3. Track selection

A track is selected if its χ^2 /*dof* is less than 2.5 and it has at least two axial and stereo segments. We do not require tracks to have a good silicon match since the proper decay lengths of the hyperons are several centimeters. The track reconstruction efficiency is a strong function of p_t and because of low track reconstruction efficiency below 0.3 GeV, only tracks with p_t above 0.3 GeV are used.

4. Reconstruction of Ks

Although Ks is not an aim of this study, it is used as a test case because the Ks invariant p_t cross section was published with Run I data[6]. The first step of the reconstruction is to take two oppositely charged good tracks and calculate their crossing coordinate in the r-ϕ plane (called the secondary vertex). Once the intersection point is found, the Z coordinate of each track (Z_1 and Z_2) is calculated at the point. If the distance between the two is less than 2.0 cm, the pair is swum back to the beam line and compared with the event vertex. If the d0 is less than 0.25 cm and the difference (δZ_0) of the Ks Z position and the event Z vertex position is less than 2.0 cm, the pair is accepted. In order to reduce the background further, it is also required that the distance between the event vertex and the secondary vertex be greater than 2.0 cm. This is the decay length (L_{Ks}) in r-ϕ plane. The cuts above are the default cuts and summarized in Table 2. The pair passing all cuts is a Ks candidate. The plots corresponding to some of the cuts are shown in Figure 1. Also shown in the same figure are those from single Ks MC data.

p_t	>.325 GeV
$\|Z_1-Z_2\|$	<1.5 cm
d0 (Ks)	<0.25 cm
δZ_0 (Ks)	<2.0 cm
decay length (L_K)	2.5 cm < L < 50 cm

Table 2. Default cuts for choosing Ks candidates.

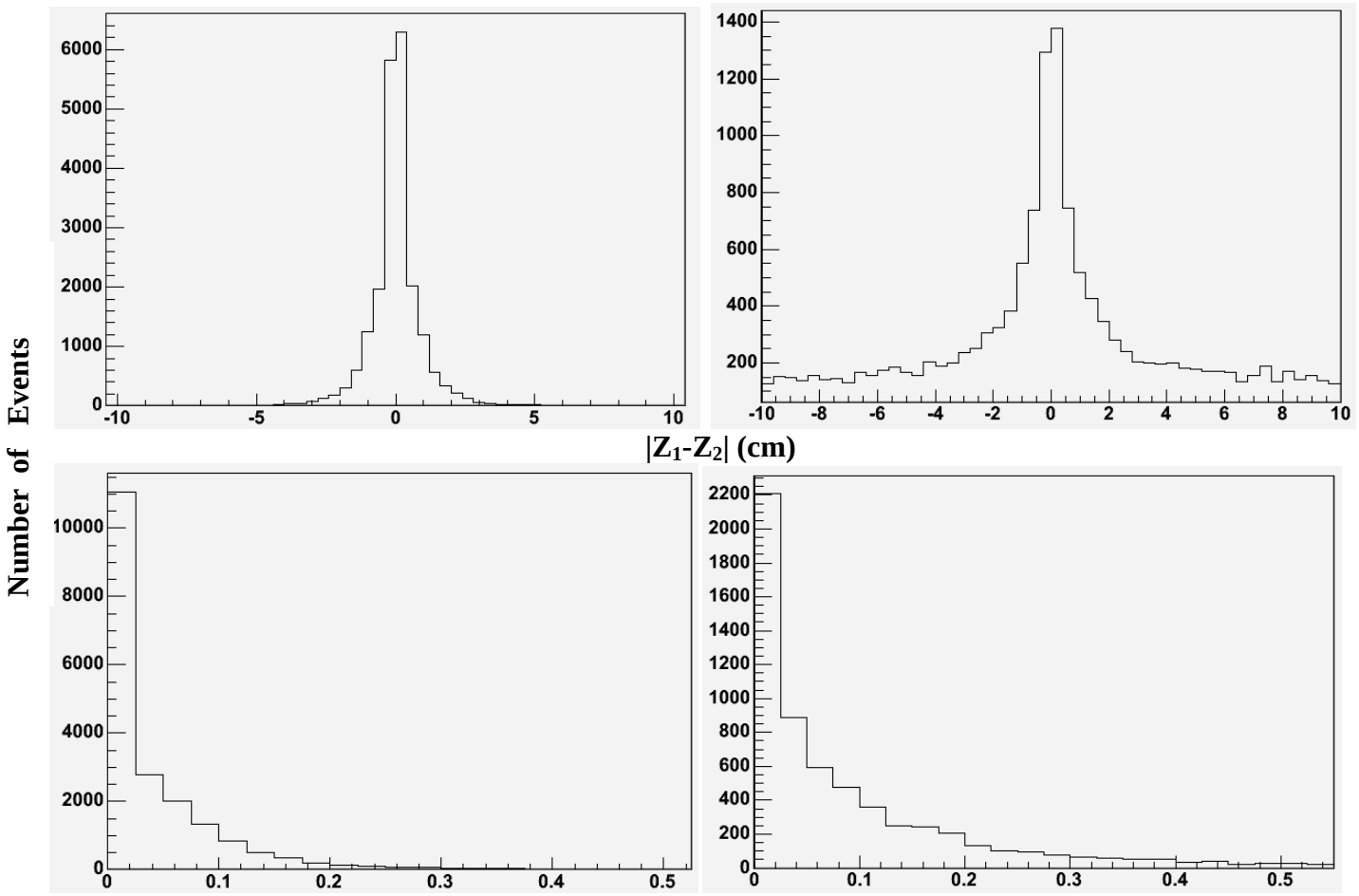

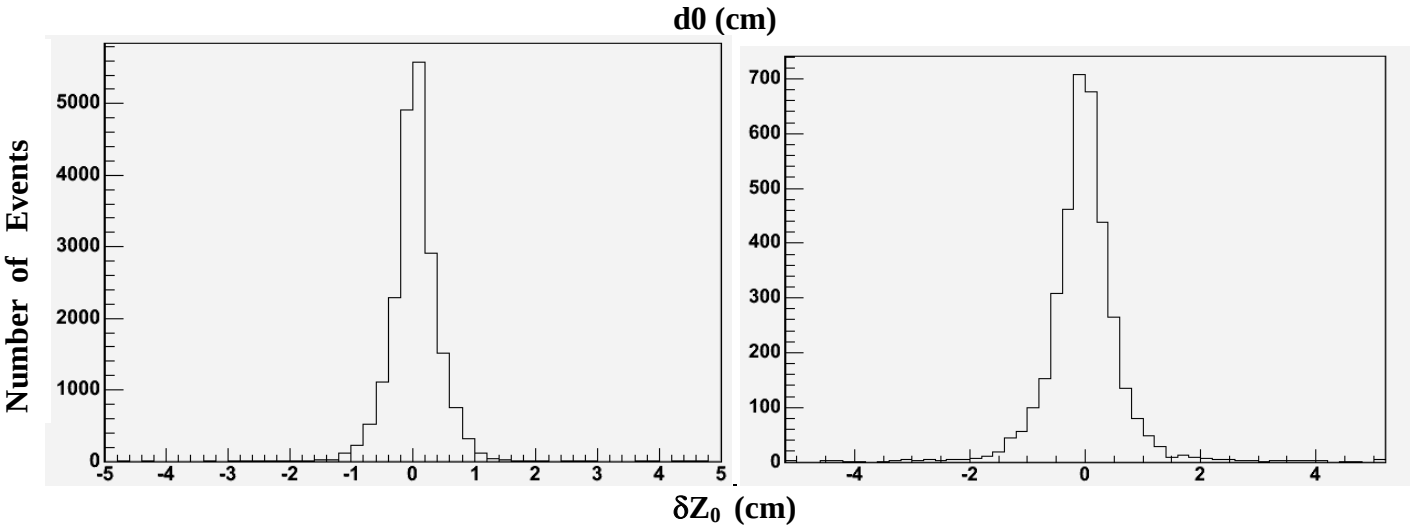

Figure 1. Plots for default variables in Table 2. Left Plots are from single Ks MC data with p_t = 2 GeV. The right plots are from real data. The top plots have L_{Ks}, and Ks mass window cut. The two bottom plots have |Z1-Z2|, L_{Ks}, and Ks mass window cut. About 25% of entries in the right bottom two plots are background.

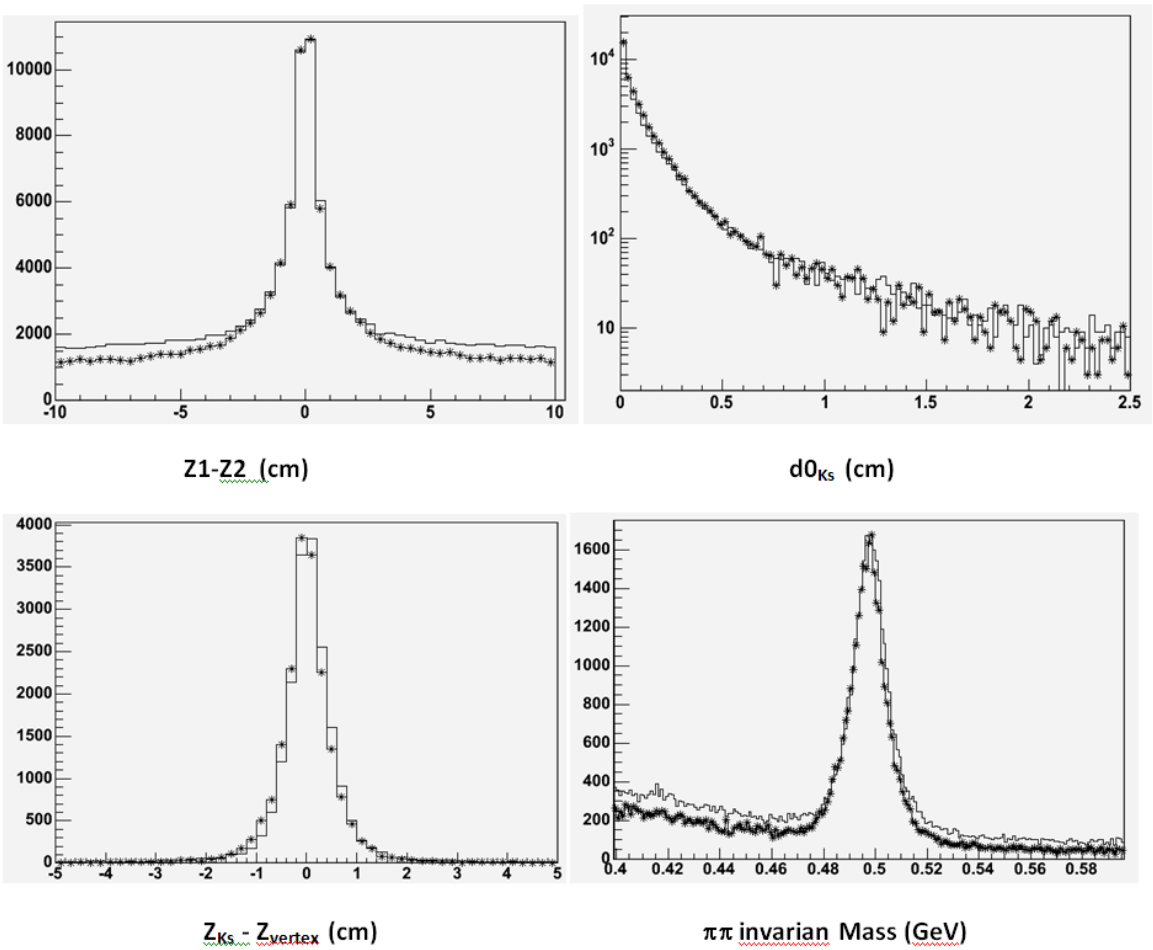

Figure 2. Comparison between PYTHIA minbiased MC data (*) and real data (histogram).

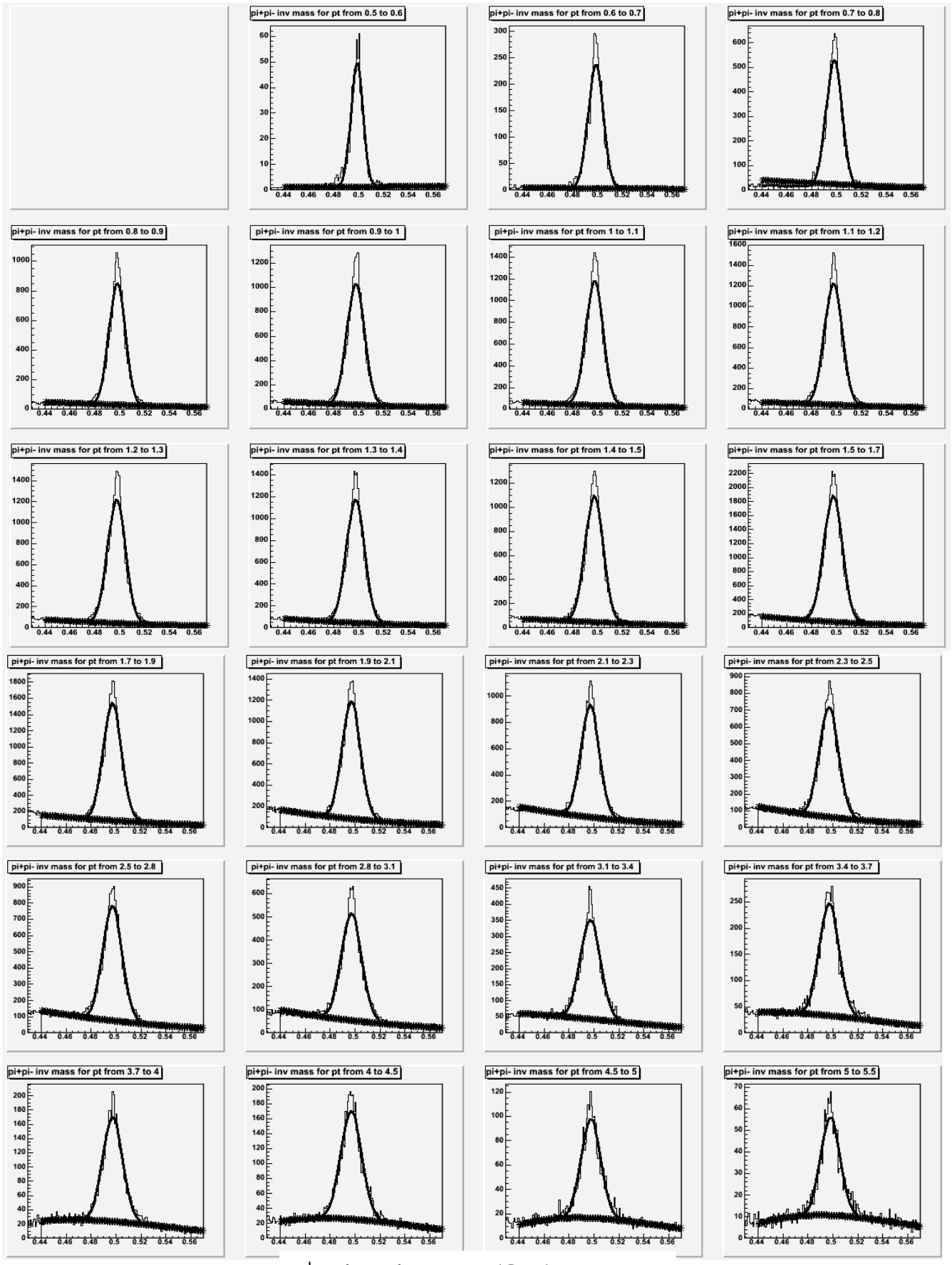

Figure 3. The invariant mass of Ks candidates for several P_t ranges, from 0.5 to 10 GeV. The horizontal axis is the $\pi^+\pi^-$ invariant mass.

As a further check of MC data, minimum biased events from PYTHIA (without any Ks mixed) are compared with real data and displaced in Figure 2. The matches are not exact because of different event characteristics, such as fraction of Ks, and average number of tracks per events.

For these Ks candidates, the invariant mass of the pair ($\pi^+\pi^-$) is plotted in Figure 3 for several p_t intervals. The mass of each track is assumed to be the pion mass. The number of Ks from each plot is obtained by fitting the plot with a Gaussian function for the peak and three degree polynomial function for the background. If the fit looks good, the polynomial background is subtracted. The number of Ks in this p_t interval is the sum of entries within the Ks mass window cut (0.480 to 0.515 GeV).

As a check on the reconstruction, the proper lifetime (in cm) is calculated. Because we cannot distinguish true Ks from background Ks on a candidate by candidate basis, the proper lifetime of Ks candidates in the signal region (within the Ks mass window, $0.480<M_{\pi\pi}<0.515$ GeV) and sideband regions ($0.43<M_{\pi\pi}<0.46$ and $0.52<M_{\pi\pi}<0.55$ GeV) are plotted and subtracted. The sideband plot is normalized to the number of background events under the Ks peak within the Ks mass window. Figure 4 shows the proper lifetime distribution for both regions and Figure 5 shows the result after the subtraction. This plot has a Ks p_t cut between 2 and 3 GeV. The 3 GeV cut is chosen because of our 50 cm decay length cut (Table 2). For a comparison, MC data with Ks pt=2 and 3 GeV are processed and the proper lifetime is plotted in Figure 6. The lifetime plots are fitted with an exponential function and 2.5 +/- 0.1 cm and 2.6 +/- 0.1cm are obtained for the real data and MC data, respectively. Although the two are consistent with each other, they are slightly lower than the PDG's 2.67 cm.

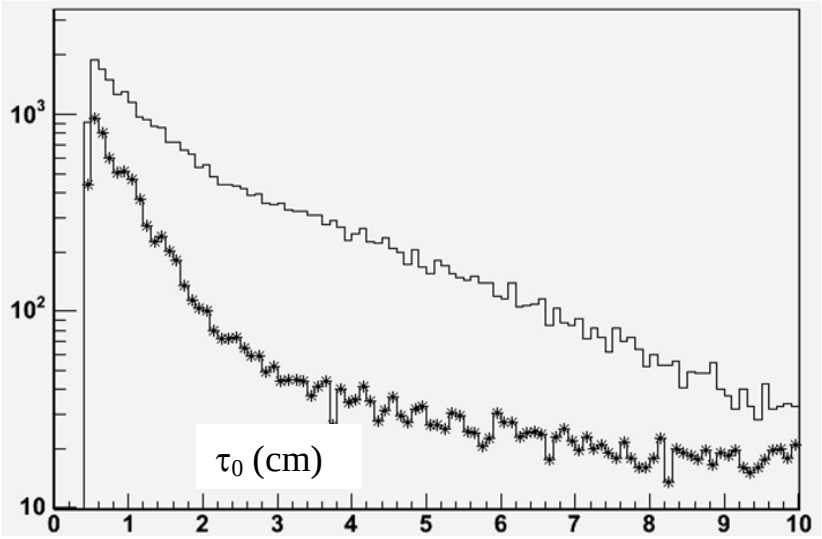

Figure 4. Proper lifetime of pairs in the signal region (Ks mass window) and side band regions. Only pairs with p_t between 2 GeV and 3 GeV are used.

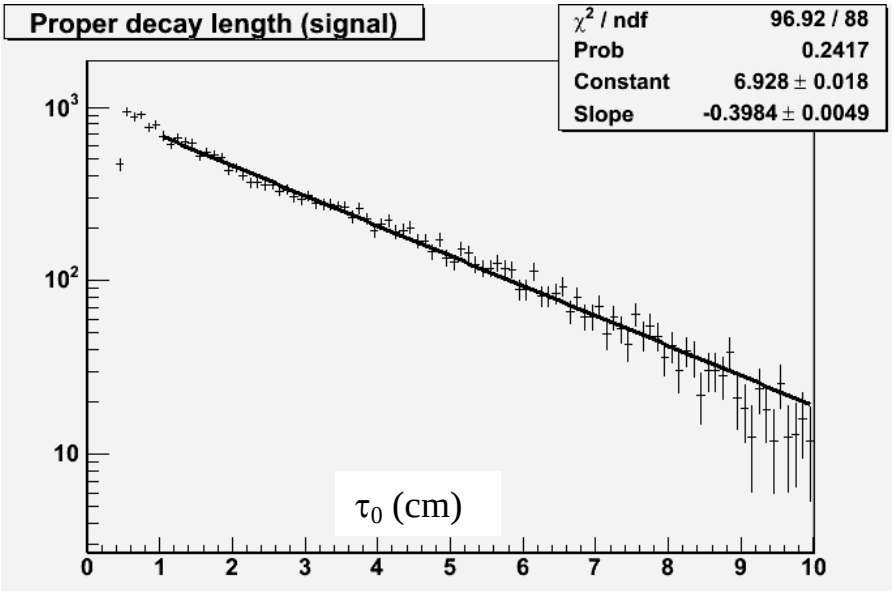

Figure 5. Proper lifetime after subtracting pairs from the side band regions.

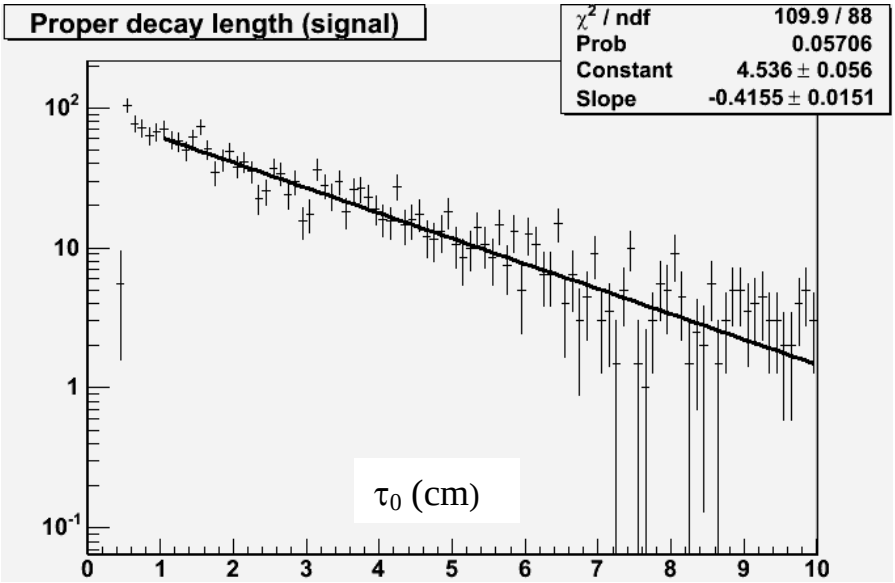

Figure 6. Proper lifetime from MC data. P_t of input Ks are 2 and 3 GeV.

Before proceeding further, let us describe how the MC data is processed. Because Ks with a fixed p_t is mixed with the PYTHIA minimum biased events, selecting out the reconstructed original Ks mixed with Ks from the minimum biased events is quite easy. Figure 7 shows the p_t distribution of the reconstructed Ks candidates passing the default cuts from MC data where 2 GeV Ks are mixed. There is a sharp peak at 2 GeV corresponding to input Ks over the background which is from Ks in the minimum biased events. Figure 8 shows the invariant mass of the candidates in Figure 7. Figure 9 shows the p_t distribution of the candidates within the Ks mass window. From the plot, we select the entries within +/-5% of the input p_t and their proper decay length is plotted as shown earlier.

Figure 9 is also used to calculate the reconstruction efficiency as a function of p_t. The background under the p_t peak is small and is estimated from p_t regions above and below the peak. The reconstruction efficiency at the p_t is the number of entries after subtracting the number of backgrounds divided by the number of input Ks. The efficiency as a function of pt shown in Figure 10 is needed to obtain the invariant p_t cross section. There are two efficiency plots. One is with one mixed minimum biased event per Ks, and the other is with four minimum biased events. The

efficiency plot with four mixed events is our default and the difference between the two is treated as one of our systematic errors. It is worthwhile to point out that the efficiency includes the branching ratio of Ks decaying to $\pi^+\pi^-$.

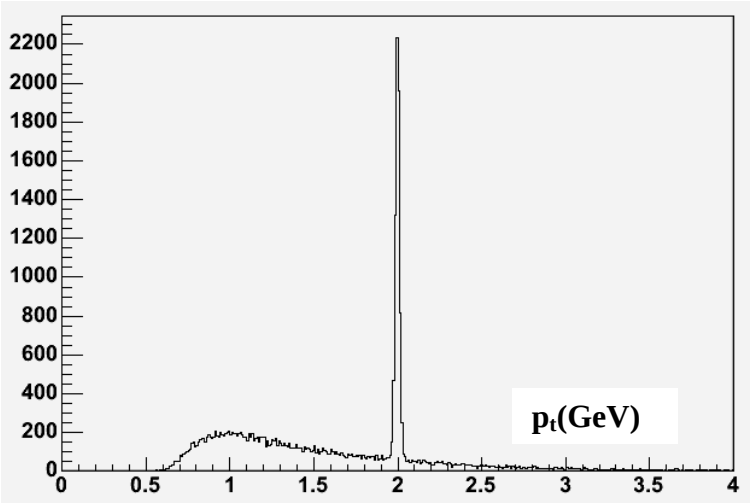

Figure 7. Reconstructed Ks candidate p_t distribution. The background is from the minimum biased events mixed with input Ks at fixed 2 GeV p_t.

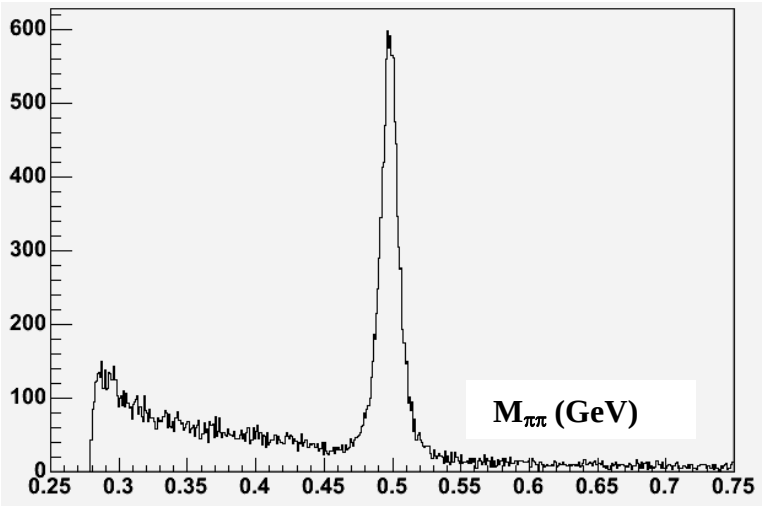

Figure 8. Invariant mass of the pairs in Figure 7.

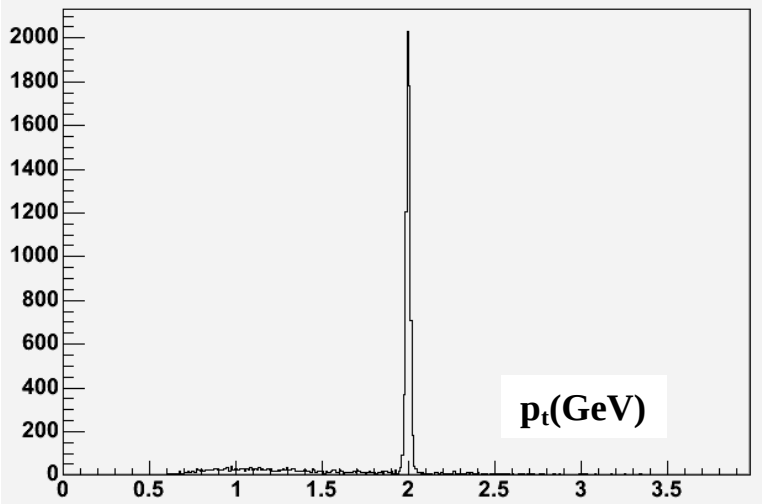

Figure 9. Reconstructed p_t distribution after making Ks mass window cut.

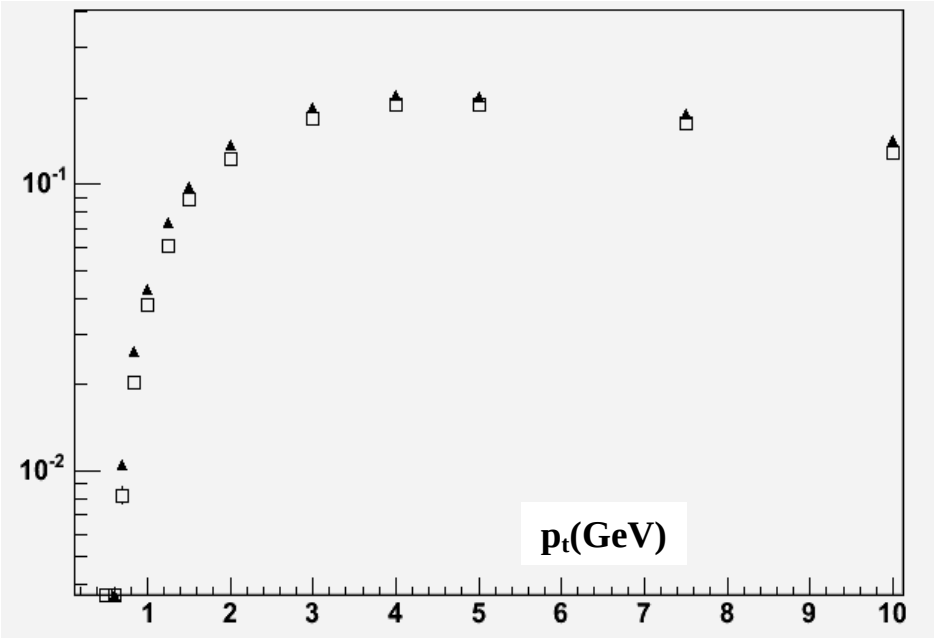

Figure 10. Efficiency curves. Square symbols are from MC data with four mixed minimum biased events and triangle symbols are from MC data with one minimum biased event.

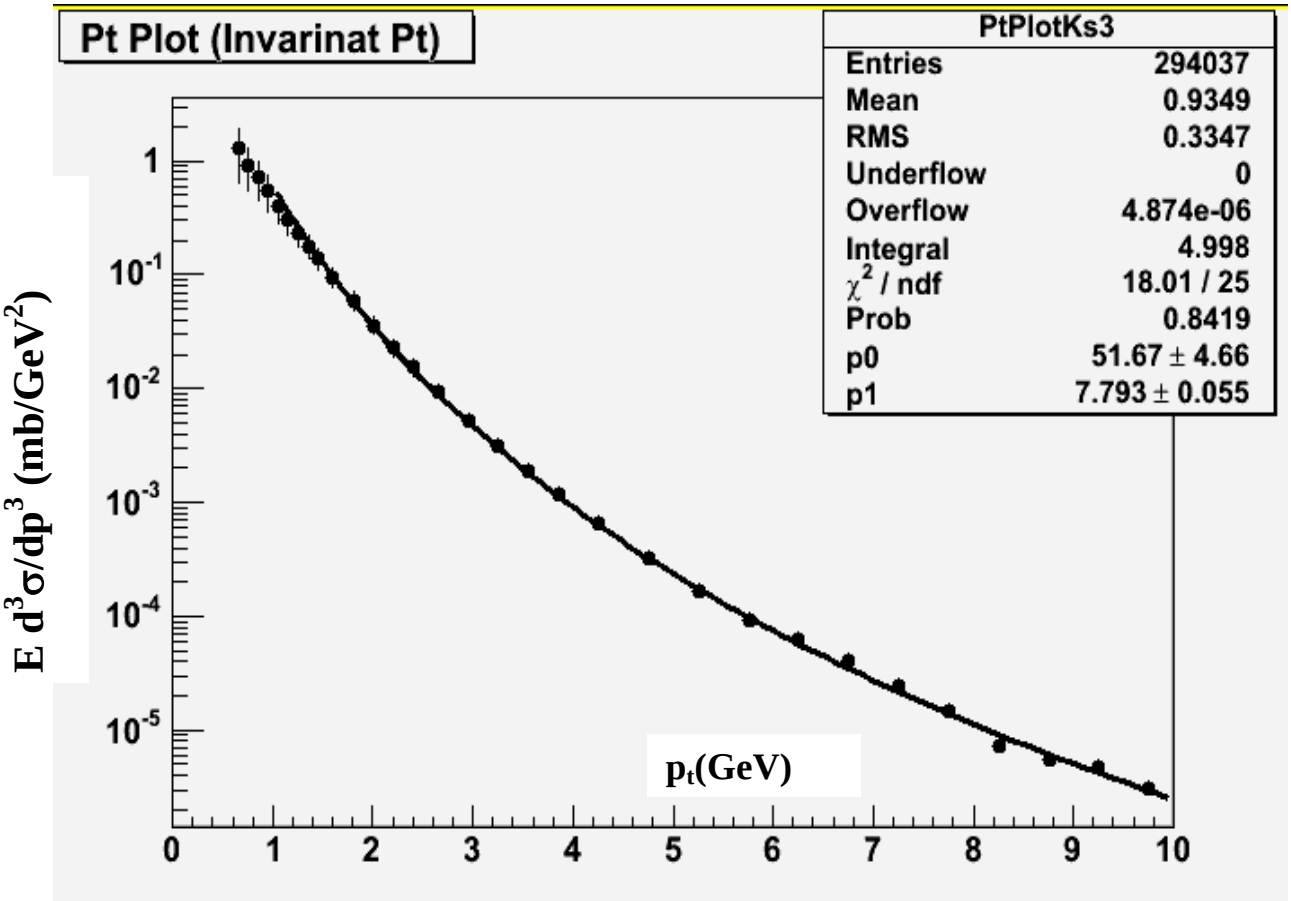

Figure 11. Inclusive invariant p_t distribution. The fitted curve is overlapped.

The invariant cross section is calculated using $Ed\sigma/dp^3 = (\sigma_t /N_t)dN/d\phi d\eta\ dp_t^2 = (\sigma_t/N_t)(1/8\pi)\ dN/p_t\Delta p_t$ where σ_t is the total $\bar{p}p$ cross section (triggered) at 1.96 TeV, N_t is the number of events used and N is the number of Ks within Δp_t divided by the efficiency at that p_t. The number of Ks is

calculated from Figure 3 as described earlier. 45mb is used for σ_t , slightly larger than 43+/-6 mb from Run I.

Figure 11 shows the Ks inclusive invariant cross section. In order to compare with the previous results, the plot is fitted with a power law function $(A)(p_0)^n /(p_t +p_0)^n$ with $p_0 = 1.3$. Table 3 shows the result from the fit. For the Ks study, the data sets with low luminosity are used.

	This analysis	Run I, PRD [6]
P_0 (fixed)	1.3	1.3
A	51.6+/-4.7	45+/-9
N	7.79+/-0.06	7.7+/-0.2

Table 3. The fitted parameters. The third column is from Run I PRD publication. P_0 is fixed for comparison purpose.

5. Luminosity correction

The data sets in Table 1 span several years of the data taking period and the instantaneous luminosity varies by ~two orders of magnitude. The average instantaneous luminosity of the gmbsbd set is $20x10^{30}$ and is $127x10^{30}$ for gmbsbm. The two plots in the right side of Figure 12 show the multiplicity distribution from data sets gmbsbd and gmbsbm. The multiplicity is the number of good tracks with $p_t > 0.30$ GeV, d0 < 0.25 cm and $\delta Z_0 < 2.0$ cm. As shown in the figure, there are more high multiplicity events in gmbsbm data set. The luminosity correction is necessary because there is somewhat weak correlation between event multiplicity and p_t of tracks in the event. The correction is done by simply weighting each event in a data set such that the multiplicity distribution from the data set follows the multiplicity distribution from low instantaneous luminosity events (left plot in Figure 12).

Figure 13 shows uncorrected invariant p_t distributions from the two data sets (gmbsbd , gmbsbm), and Figure 14 shows the same but after the correction is applied. The two after the correction match much better.

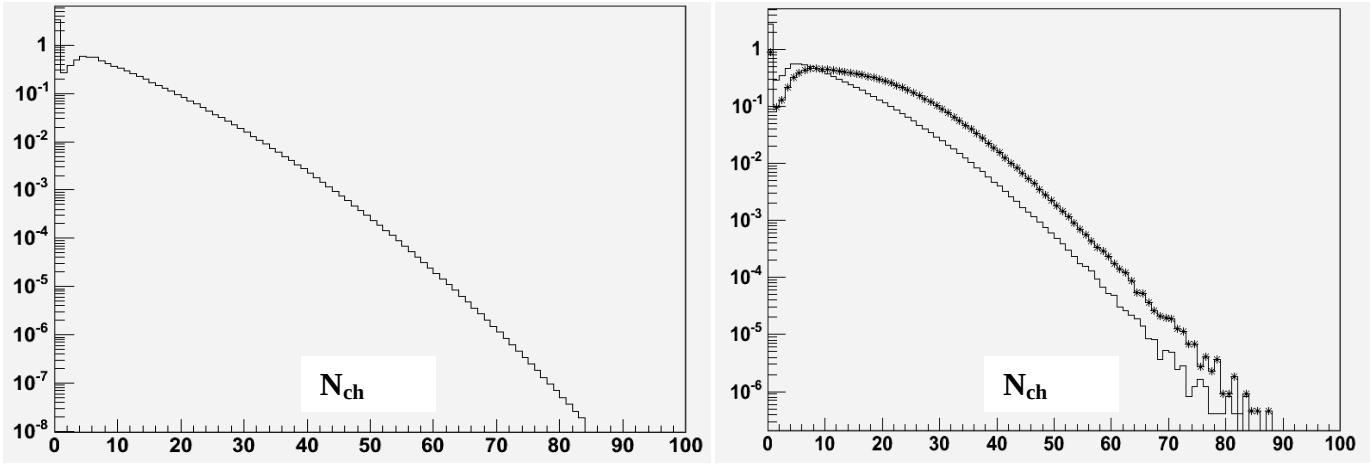

Figure 12. Left: Multiplicity distribution of events with instantaneous luminosity less than 10^{31}. Right: Multiplicity distribution from low(histogram, gmbsbd) and high luminosity (*, gmbsbm) data set.

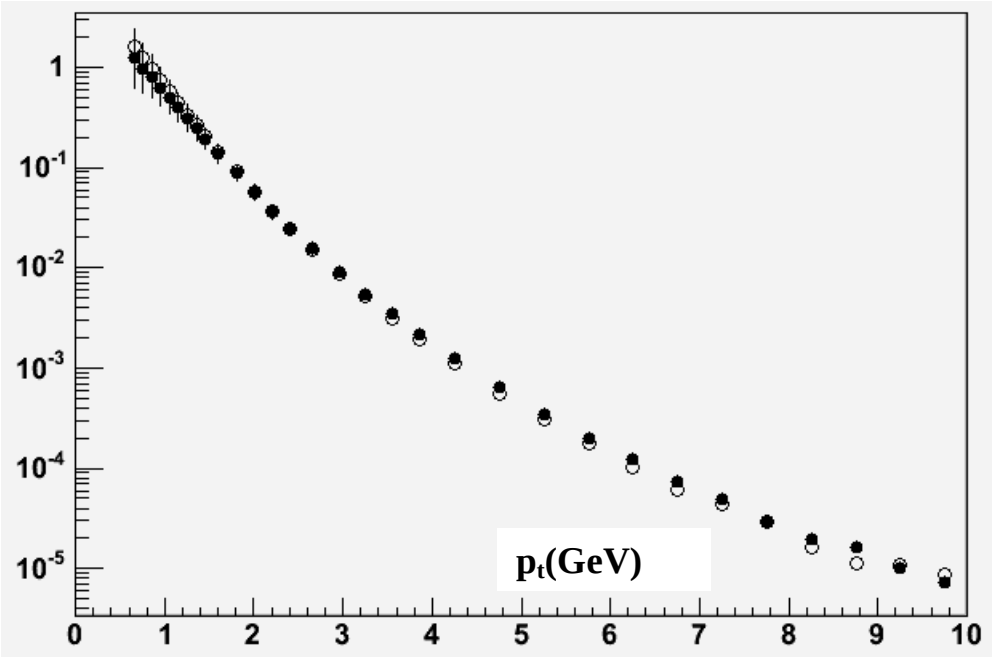

Figure 13. p_t distribution, uncorrected.

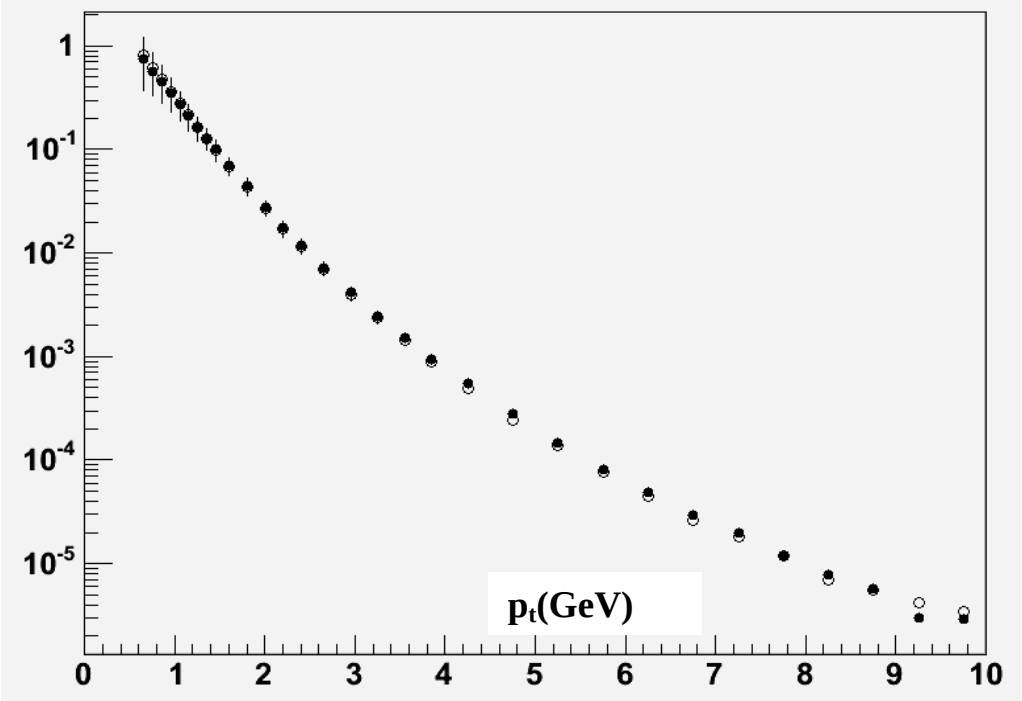

Figure 14. p_t distribution, corrected.

6. Systematc errors

The data points in the p_t distributions (Figure 11, 13 and 14) include the systematic errors, and the errors are estimated by changing the default values in Table 2. A detailed discussion is presented in the lambda section.

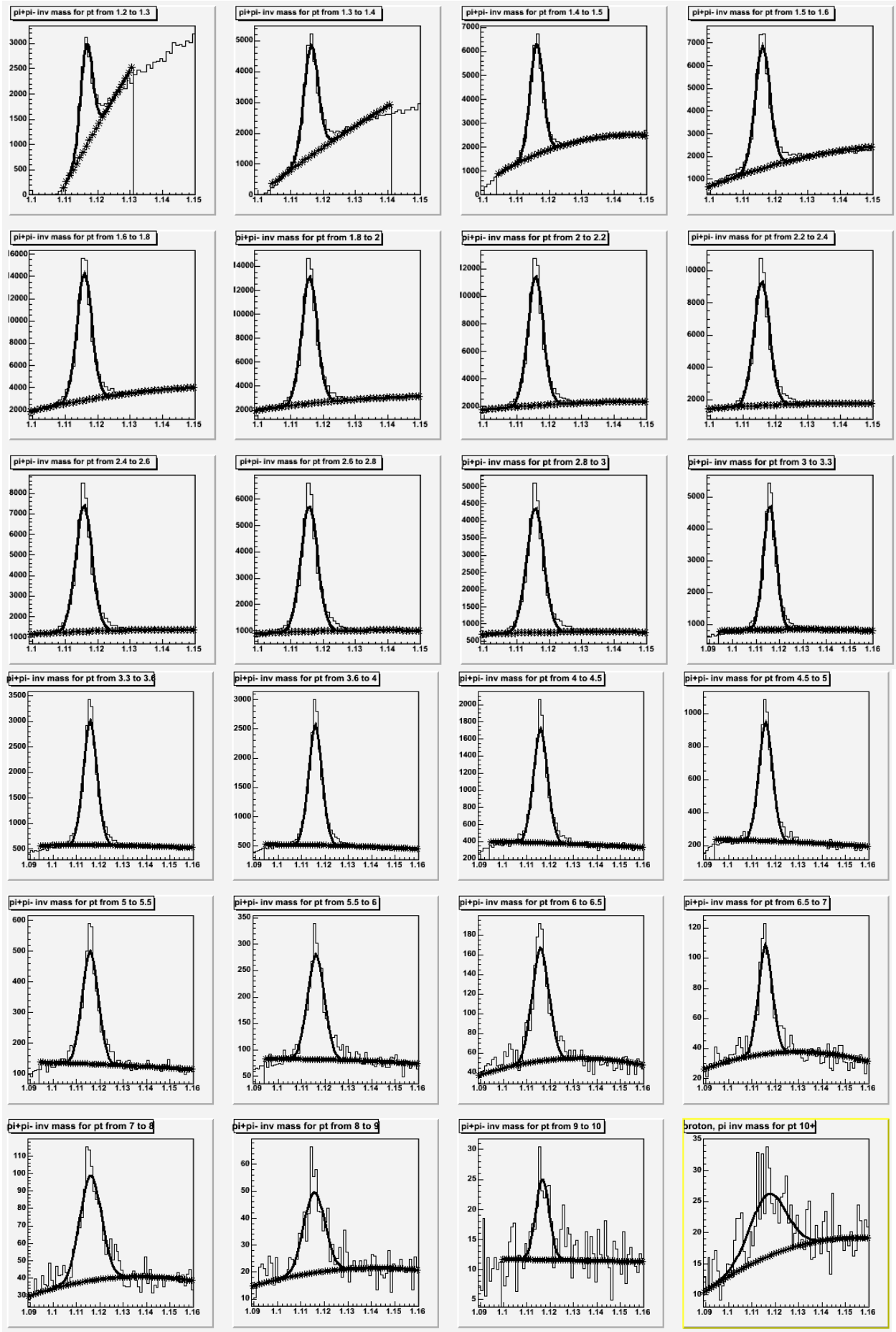

Figure 15. Proton and π^- plus anti-proton and π^+ invariant mass distribution.

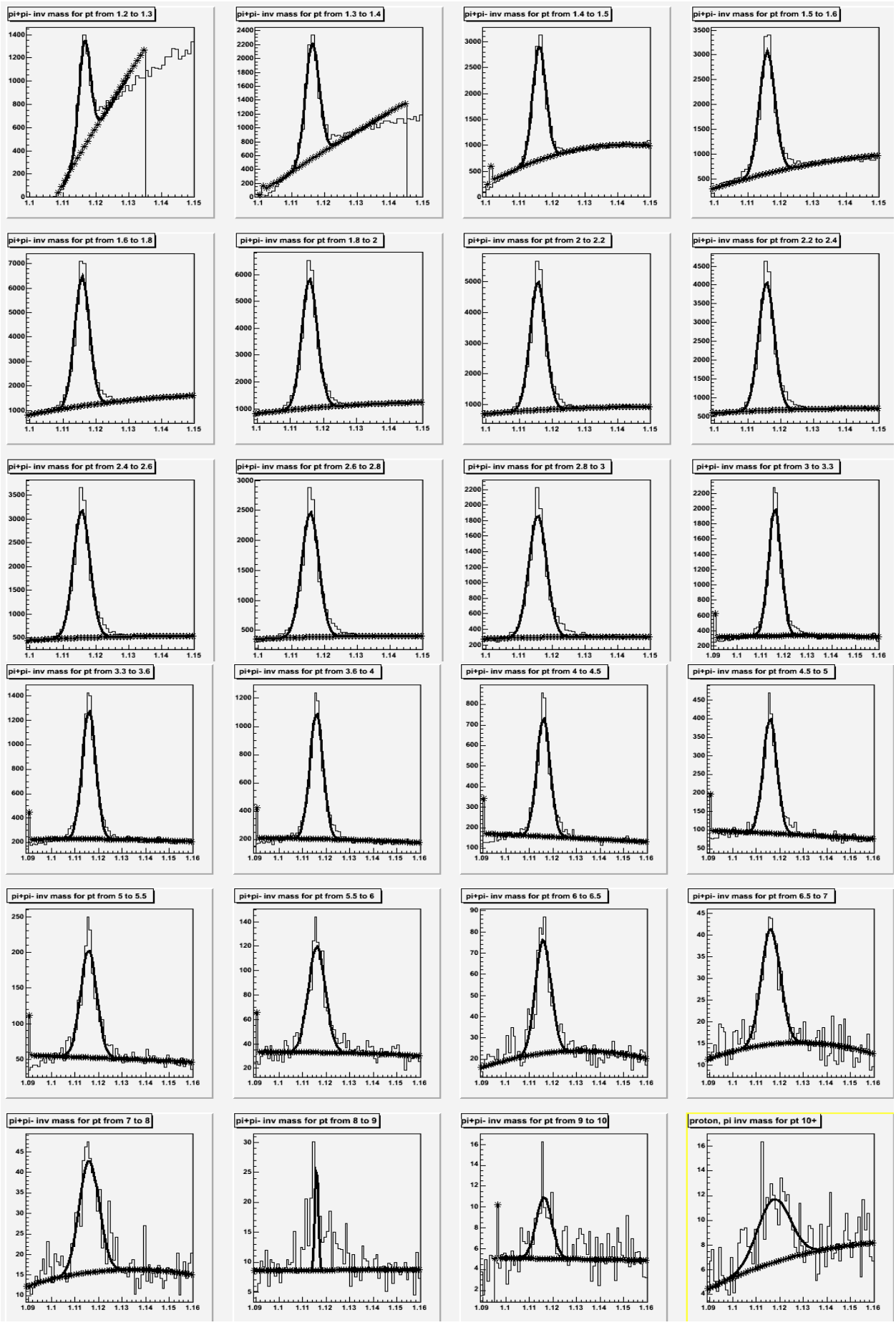

Figure 16. Proton and π^- invariant mass distribution.

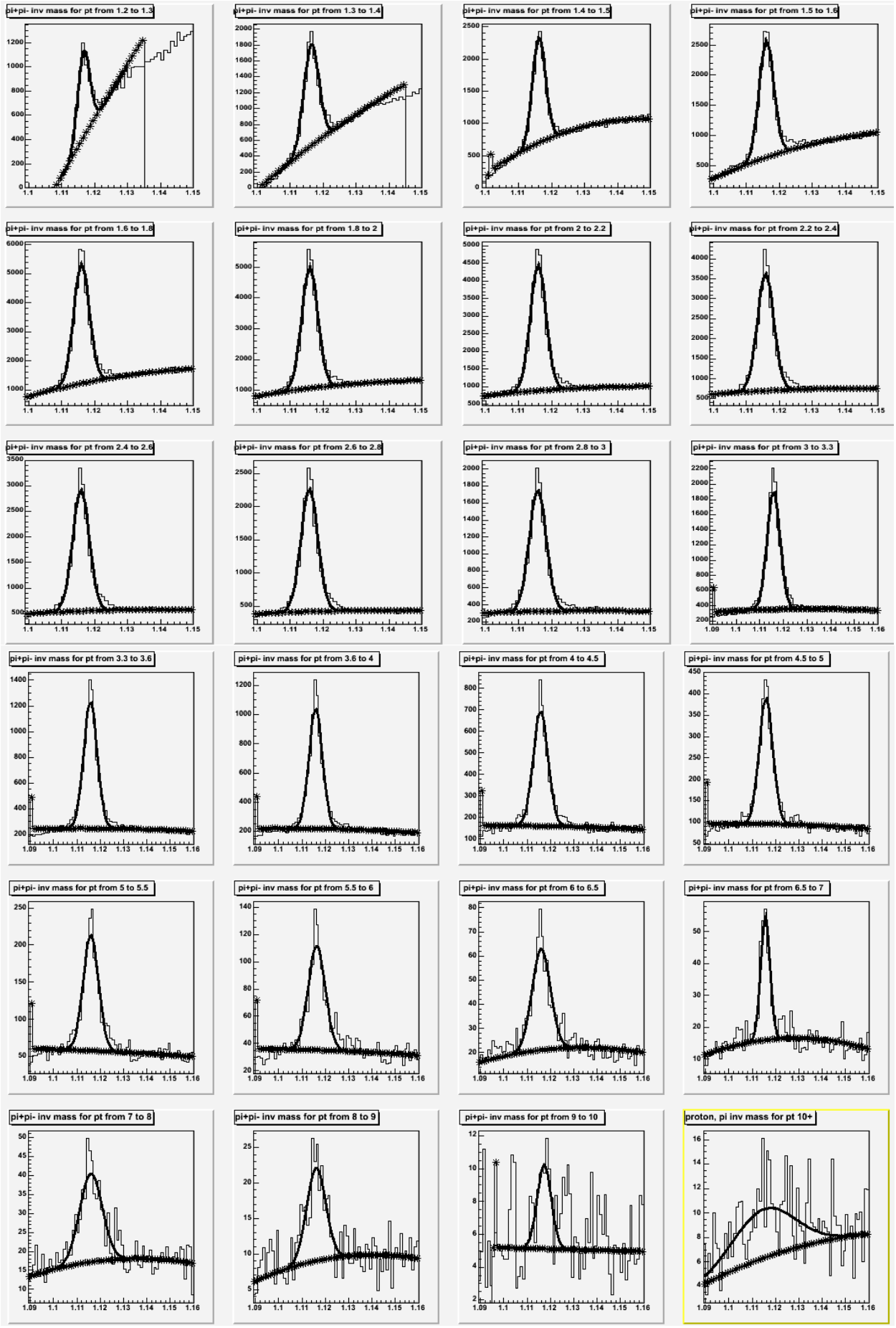

Figure 17. Anti-proton and π^+ invariant mass distribution.

7. Lambda reconstruction.

The lambda reconstruction is similar to the Ks reconstruction. For a lambda reconstruction which decays to a proton and a pion, the track with higher momentum is assigned the proton mass, which is kinematically true. Figure 15 shows the invariant mass plots of lambdas plus anti-lambdas after the default cuts (Table 2) for several p_t ranges. "Lambda" normally represents both lambda and anti-lambda. When they have to be separated out, the distinction is made explicitly. This will be also the case for "cascade" and "omega". Figure 16 shows the same for only lambdas and
Figure 17 is for anti-lambdas. As in the Ks invariant cross section calculation, each plot is fitted with a Gaussian plus a three degree polynomial function. The polynomial background is subtracted and the number of lambdas for the pt range is calculated. This number is efficiency corrected and the invariant p_t cross section is calculated and shown in Figure 18. Because the lambda efficiency and anti-lambda efficiency are not the same, the average efficiency of the two as a function of p_t is used. The two efficiency plots are shown in Figure 19. Figure 20 shows the invariant p_t cross section of lambdas and anti-lambdas separately, and the two match fairly well.

Figure 21 shows the proper lifetime for lambda candidates within the lambda mass window ($1.111<M_{p\pi}<1.121$ GeV) and sideband windows ($1.095<M_{p\pi}<1.105$ and $1.125<M_{p\pi}<1.135$ GeV). The lifetime from the sidebands is normalized to the background under the lambda peak. Only those with p_t between 2 and 3 GeV are used. Figure 22 shows the lambda proper lifetime after the background is subtracted. The plot is fitted with an exponential function and 7.5 cm is obtained for the lifetime. Figure 23 shows the same from MC data and its lifetime is 7.5 cm. Compared to the 7.8 cm PDG value, both are slightly low. The structures in the plots are likely the material effect.

As mentioned briefly in the Ks section, the systematic error as a function of p_t is calculated by changing the default cut values. Table 4 shows the variations of the default values in Table 2. For each variation, the efficiency curve as a function of p_t is re-calculated and the corresponding invariant cross section is obtained. In order to estimate the total systematic error as a function of p_t, the new invariant cross section is divided by the same obtained with default cuts. This is called the ratio, $R_i(p_t)$, for i^{th} variation. Figure 24 shows $R_i(p_t)$ for all variations. The total systematic error at a p_t is the square root of the quadratic sum of (R_i-1) and is shown in Figure 25.

	Default	Variation 1	Variation 2
p_t	.325 GeV	.300 GeV	.350 GeV
$\|Z_1-Z_2\|$	1.5 cm	1.0 cm	2.5 cm
d0 (Ks)	0.25 cm	0.10 cm	-
δZ_0 (Ks)	2.0 cm	5.0 cm	-
decay length (L_{Ks})	2.5 cm <L<50 cm	1.0 cm <L<50 cm	5.0 cm <L<50cm
Number of Mix	four events	One event	-

Table 4. The variations from default values for the systematic error estimation.

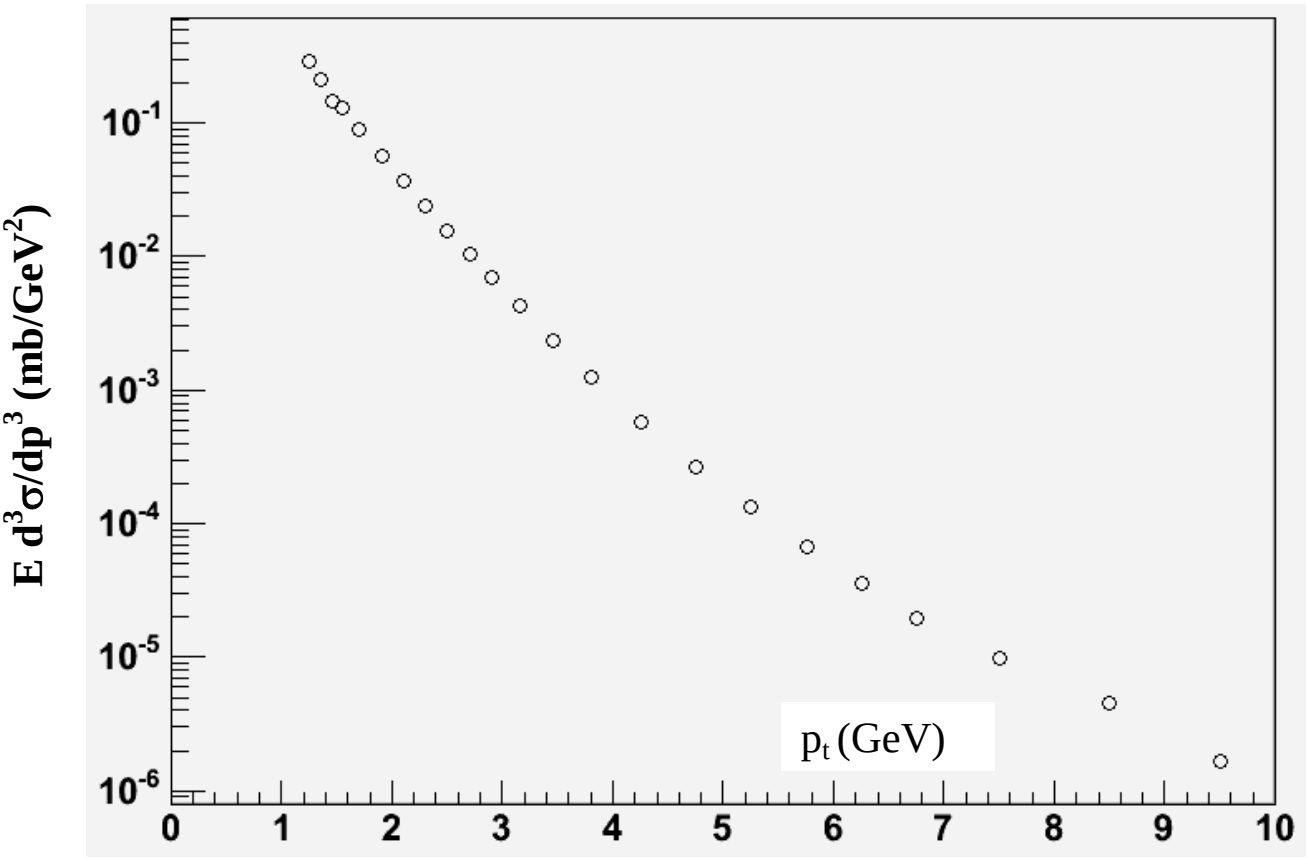

Figure 18. Invariant p_t cross section of lambdas plus anti-lambdas.

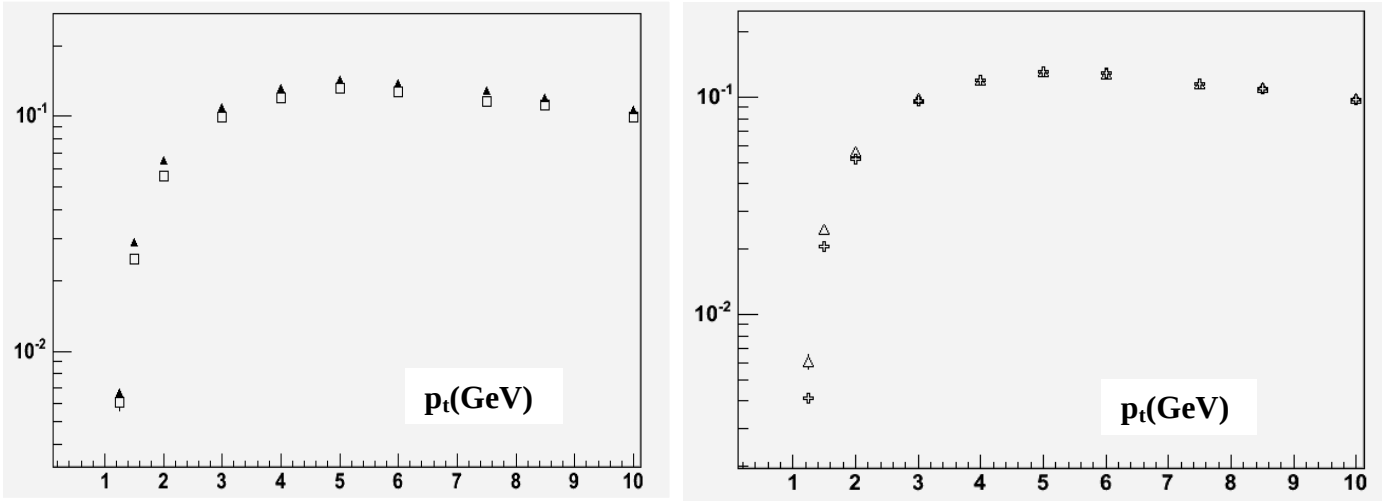

Figure 19. Reconstruction Efficiency. Left plot: triangles (squares) are with one (four) MB mixed. Right plot: triangles are for lambda reconstruction efficiency, and crosses are for anti-lambda efficiency.

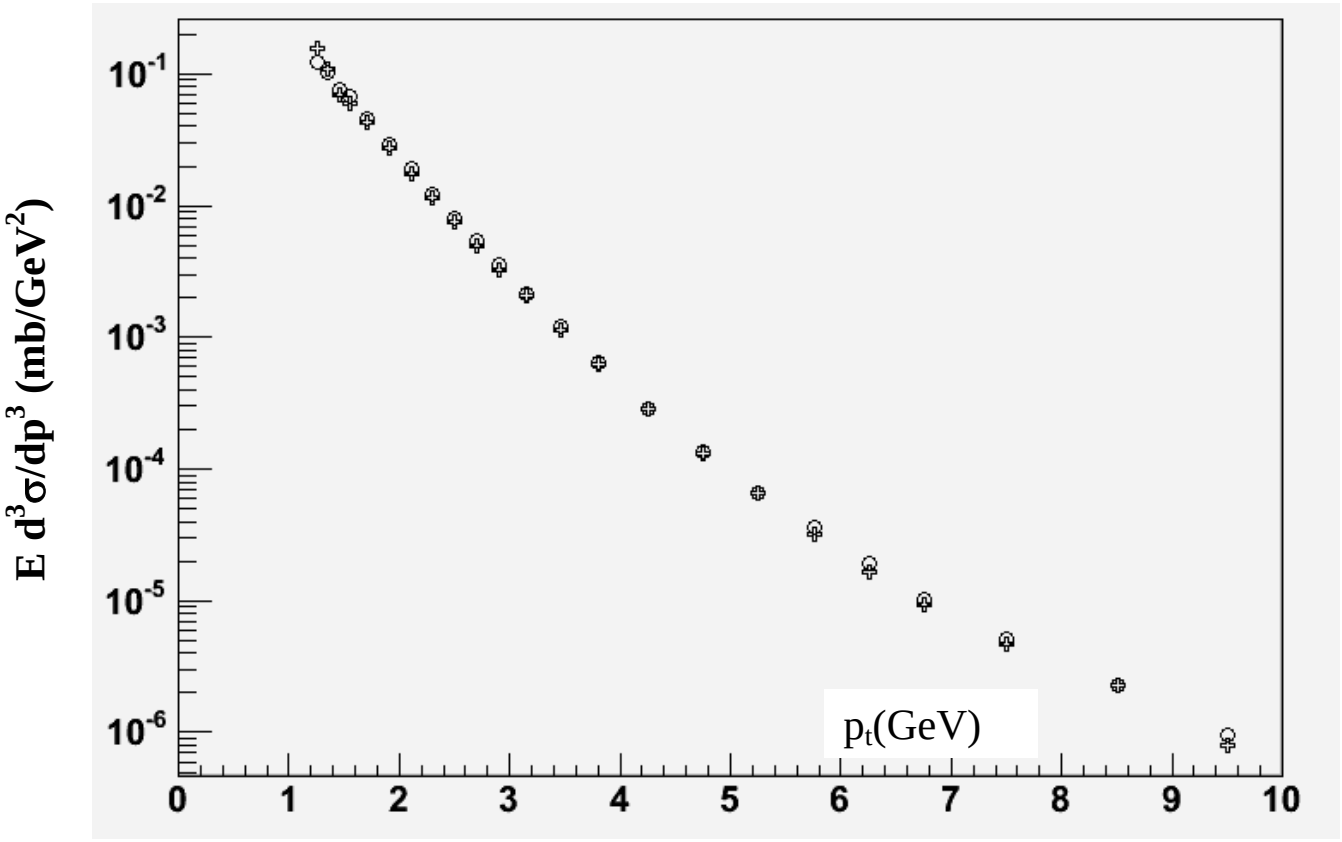

Figure 20. Invariant p_t cross section of lambdas (circles) and anti-lambdas (crosses) separately.

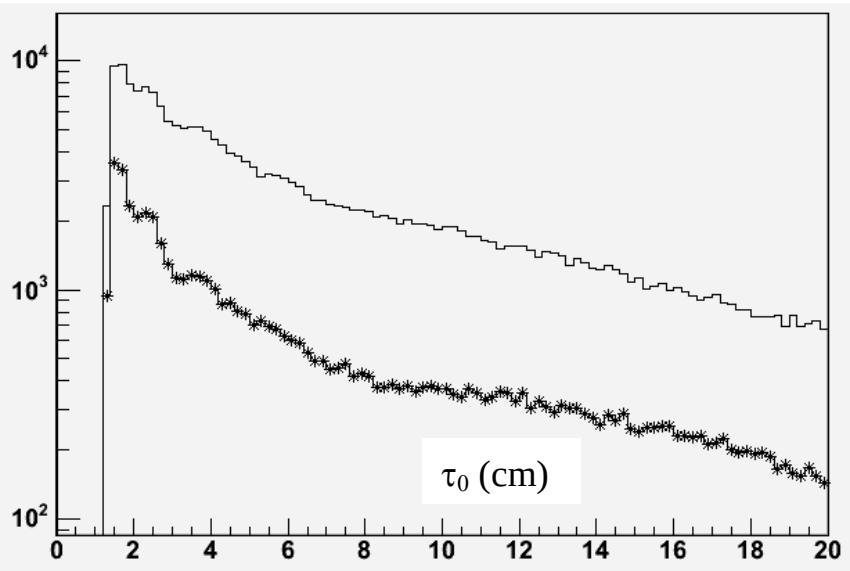

Figure 21. Proper life time of lambda candidates from the signal region and sideband regions. Only pairs with p_t between 2 and 3 GeV are used.

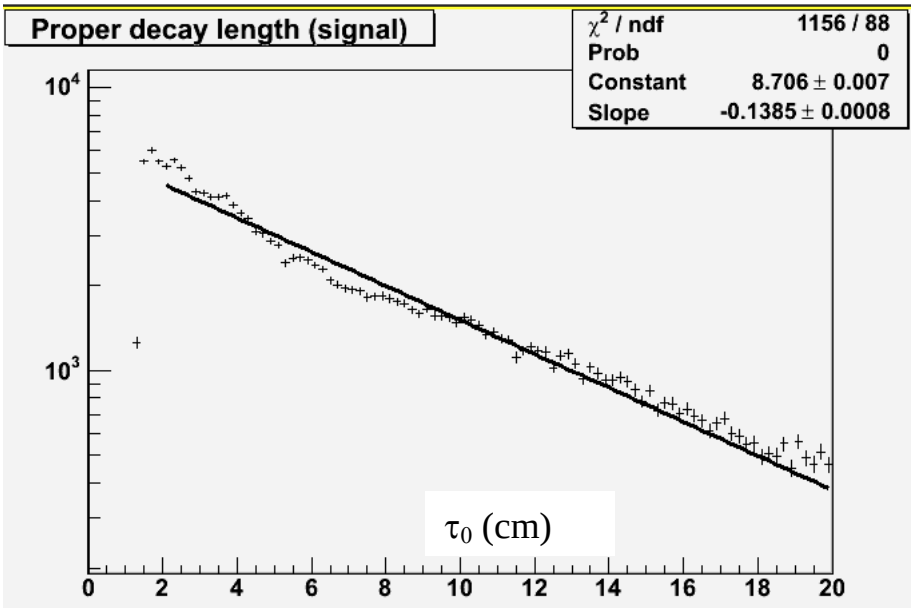

Figure 22. Proper lifetime of lambdas after subtracting the sideband contribution.

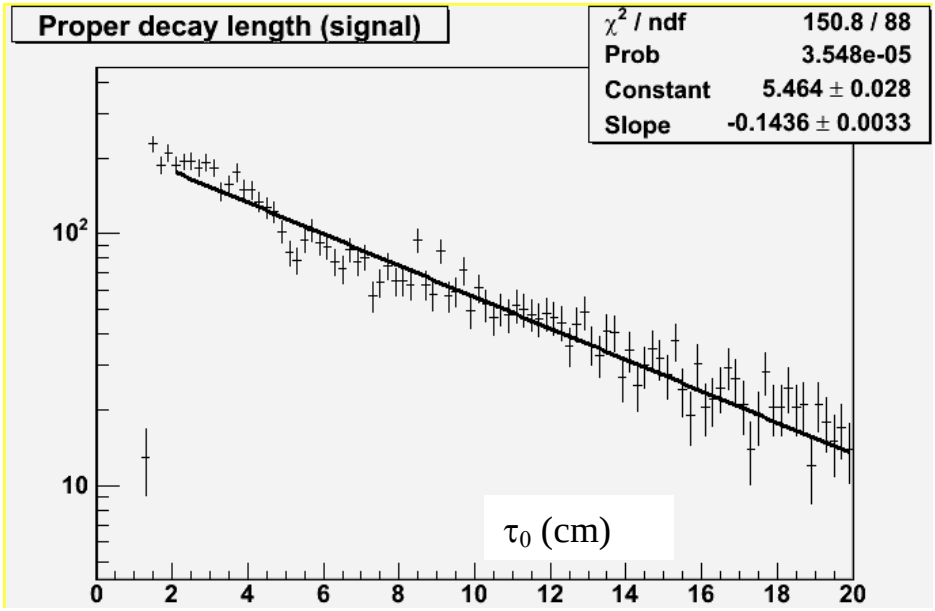

Figure 23. Lambda proper lifetime from MC events. The MC data is with 2 and 3 GeV lambdas.

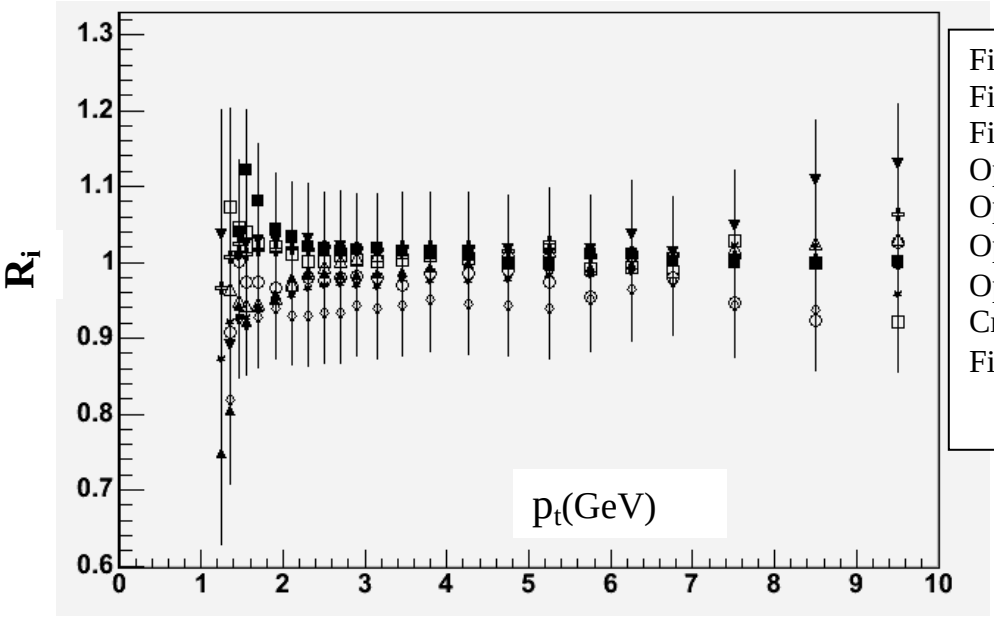

Filled square : pt> 0.35 GeV
Filled triangle : pt>0.30 GeV
Filled inverted triangle : 1 MB mixed
Open circle : |z1-z2| <2.5 cm
Open square : |z1-z2| <0.75 cm
Open triangle : L_Λ >1.0 cm
Open diamond : L_Λ > 5 cm
Cross : d_0 <0.10 cm
Filled star : δz_0 <5.0cm

Figure 24. R_i (p_t) distribution (ignore error bars).

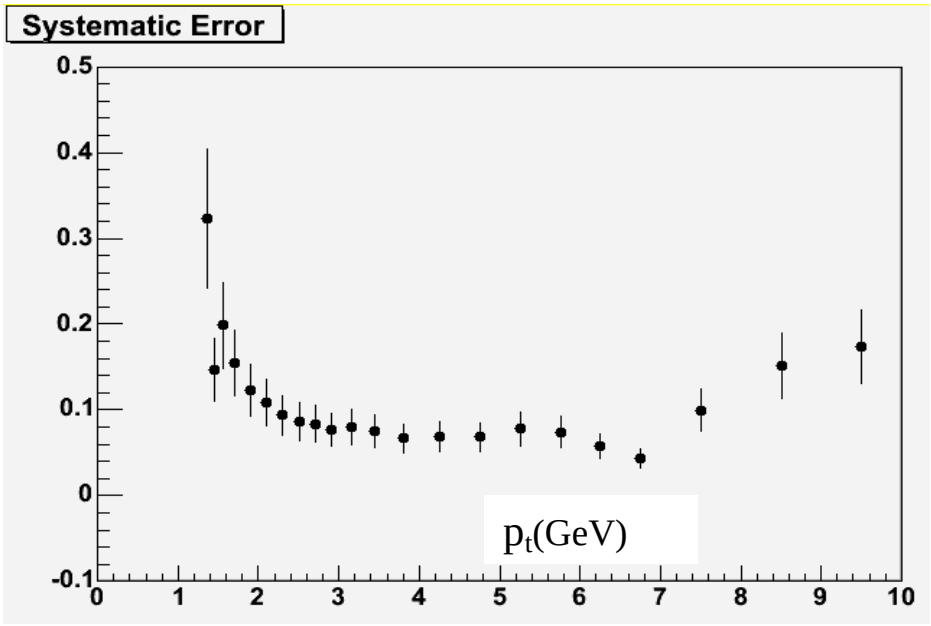

Figure 25. Lambda systematic error as a function of p_t.

8. Cascade reconstruction

The cascade reconstruction decay mode is $\Xi^- \rightarrow \Lambda\pi^- \rightarrow (p\pi^-)\pi^-$ (and $\Xi^+ \rightarrow \bar{\Lambda}\pi^+ \rightarrow (\bar{p}\pi^+)\pi^+$). Lambdas previously constructed are used to reconstruct cascades. First the lambda candidates with invariant mass between 1.111 and 1.121 GeV before d0 and δZ_0 cuts are applied. This is because some lambdas from cascades may likely miss the vertex cuts. For each lambda candidate, the coordinate of the intersection point between the candidate and another track (third track) is calculated in r-ϕ space. Once the intersection point is found, the Z coordinates are calculated at the point (Z_3 for the third track and Z_4 for lambda candidate). If the distance between the two ($|Z_3-Z_4|$) is less than 1.5 cm the candidate and the third track are combined and swum back to the beam line and compared with the event vertex. The third track is assigned a pion mass.

There are two decay lengths for cascades. One is the lambda decay length and the other is the cascade decay length. We require the lambda decay length to be greater than 2.5 cm and the cascade decay length to be greater than 1cm. Moreover, since lambdas are from cascades, we also require the difference between the lambda decay length and cascade decay length to be greater than 0.5 cm.

The final cut is the event vertex cut. Similar to the Ks case, if d0 is less than 0.25 cm and the distance to the event Z vertex is less than 2.0 cm, it is a cascade candidate.

The cuts are summarized in Table 5.

p_t	>.325 GeV
$\|Z_1-Z_2\|$	<1.5 cm
decay length (L_Λ)	2.5 cm < L < 50 cm
$\|Z_3-Z_4\|$	<1.5 cm
Decay length (L_Ξ)	>1.0 cm
$L_\Lambda - L_\Xi$	>1.0 cm
d0 (Ξ)	<0.25 cm
δZ_0 (Ξ)	<2.0 cm

Table 5. Cuts for cascade selection.

The invariant masses of the candidates passing all cuts are plotted (Figure 26 for cascades, Figure 27 for anti-cascades and Figure 28 for the sum of the two) for several p_t intervals.

These plots are fitted as Ks and lambda cases and the number of cascades is found and efficiency corrected. The cascade mass window is 1.31 to 1.33 GeV.
Figure 29 shows efficiency plots for cascades and anti-cascades separately, and Figure 30 shows the invariant p_t cross section for cascades and anti-cascades separately. As in the case of lambdas, the match is fairly good. Figure 31 shows the cross section of cascades together with anti-cascades. The average efficiency of cascades and anti-cascades is also used.

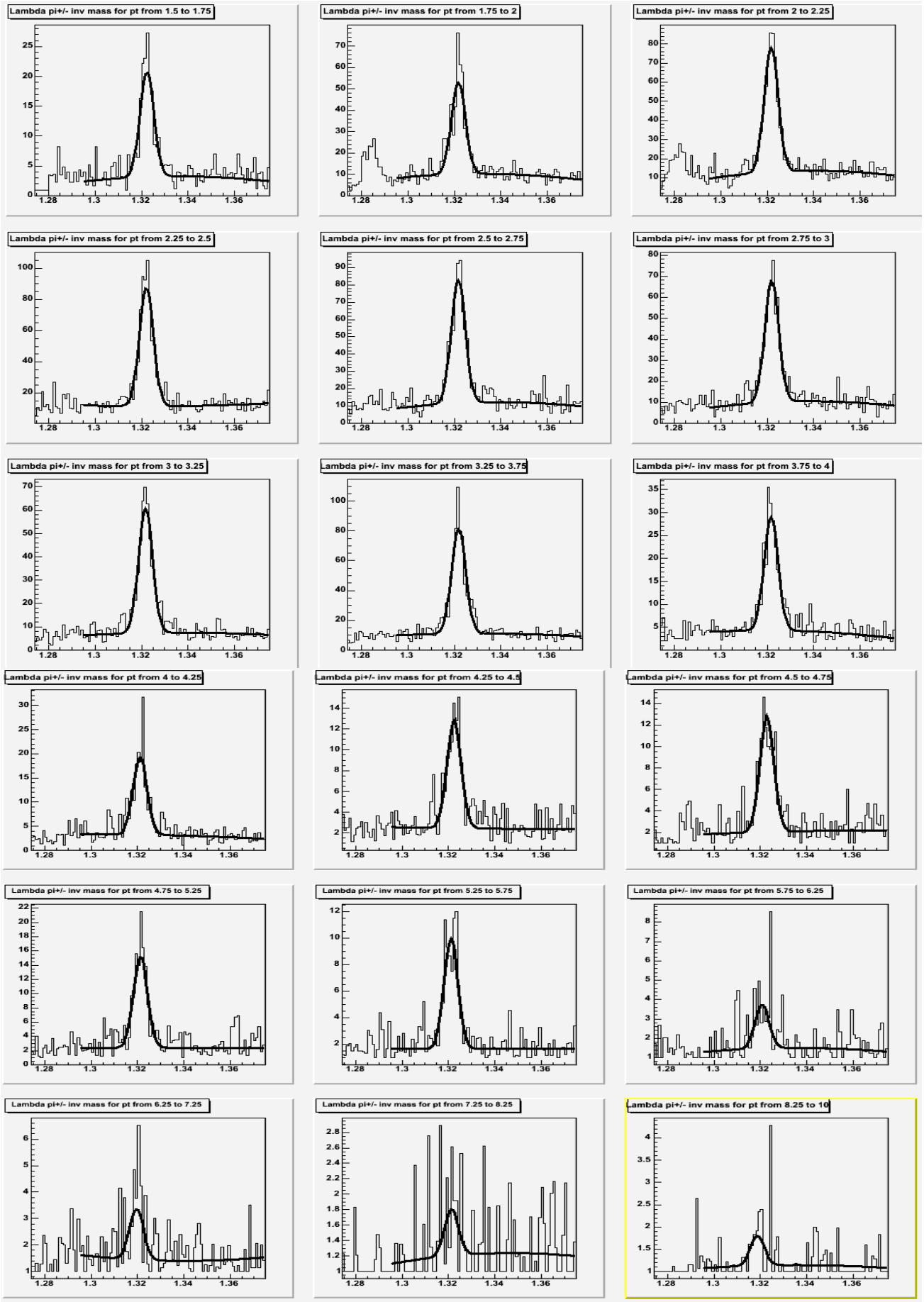

pππ invariant mass (GeV)

Figure 26. Invariant mass of cascade candidates.

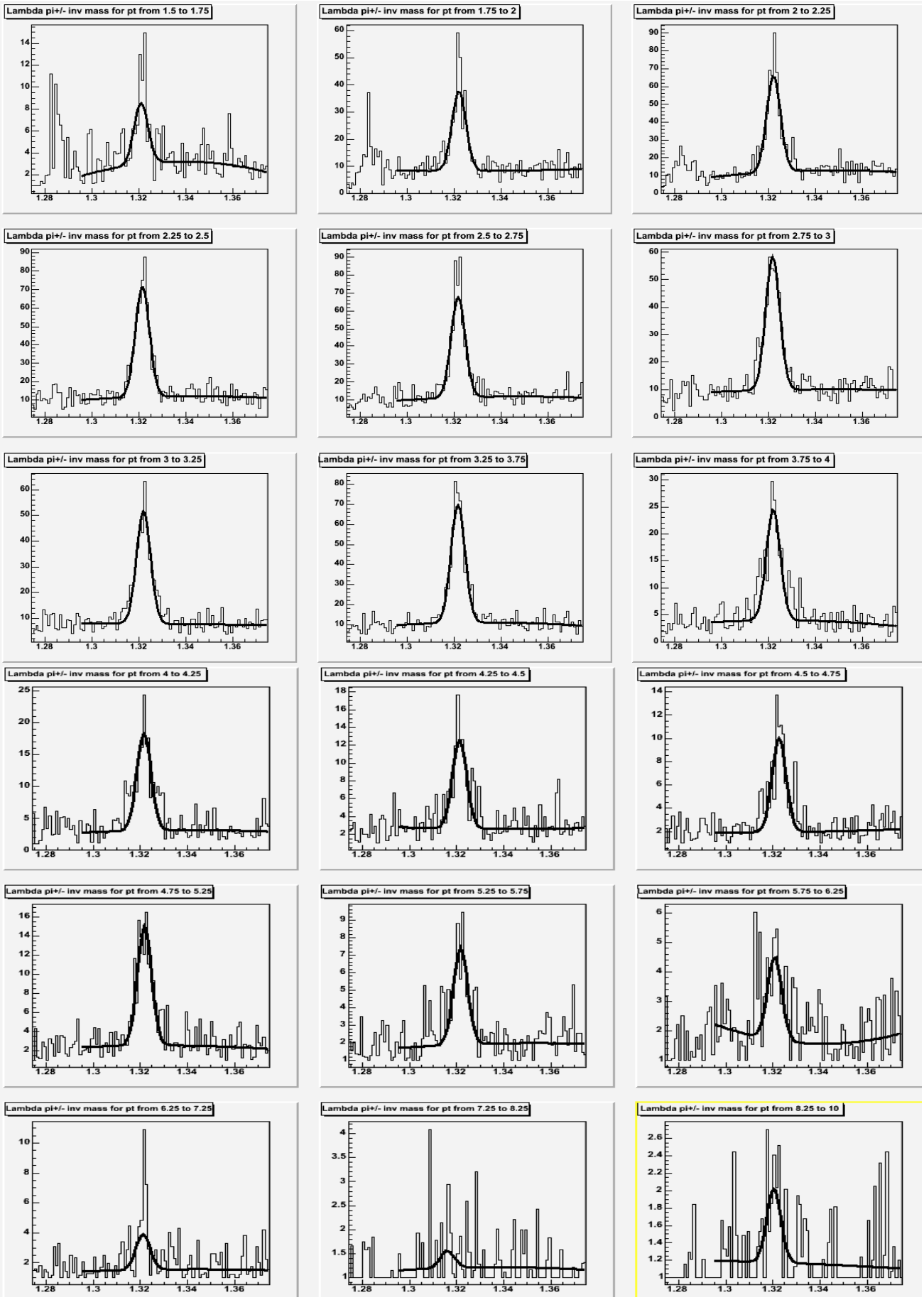

pππ invariant mass (GeV)

Figure 27. Invariant mass of anti-cascade candidates.

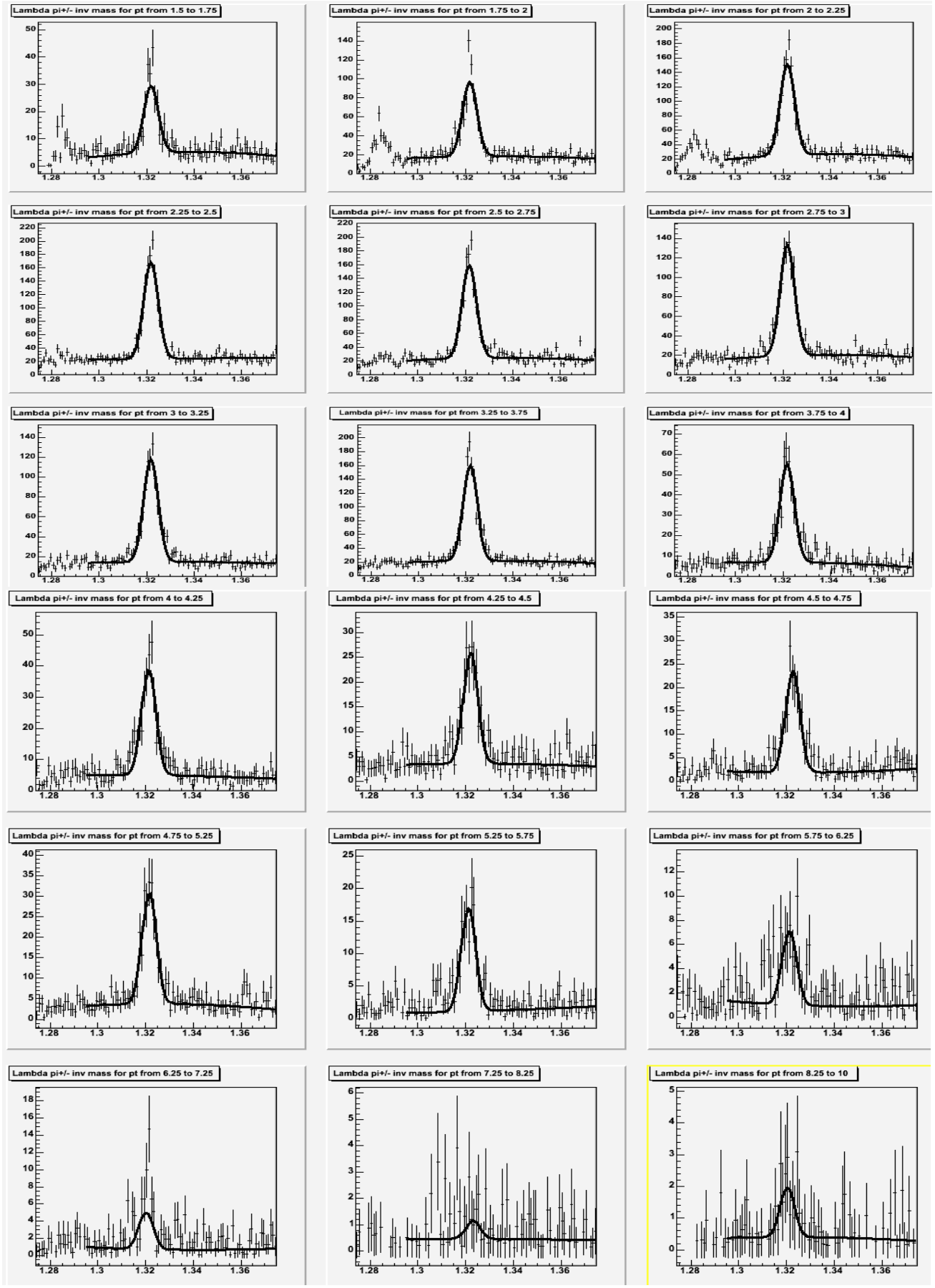

Figure 28. Invariant mass of cascade plus anti-cascade candidates.

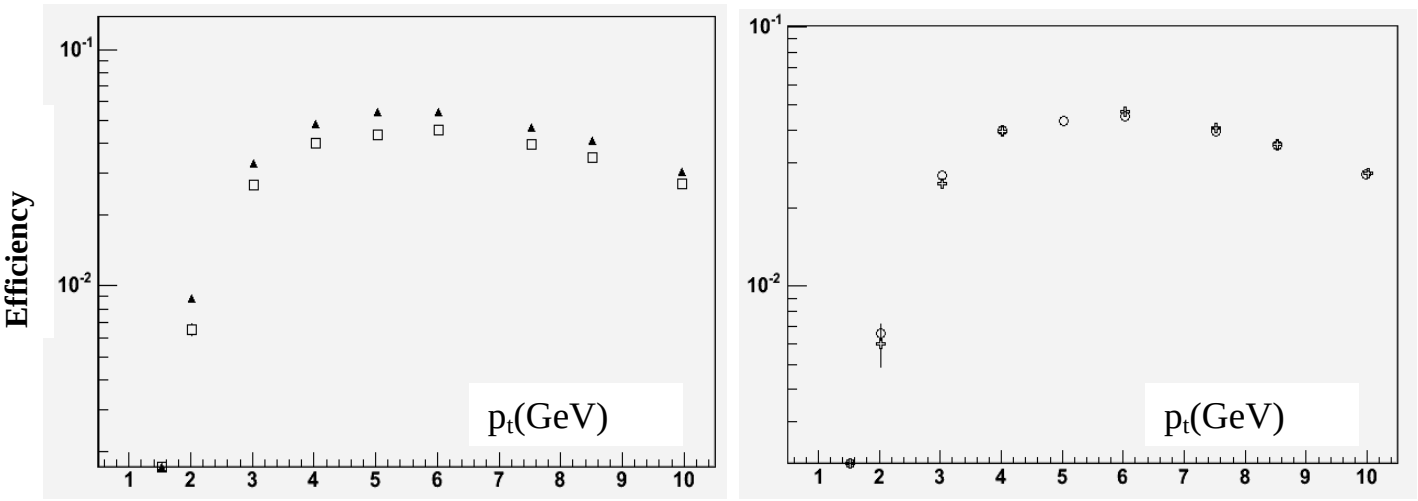

Figure 29. In the left plot, triangle (square) symbols are with one (four) MB event. In the right plot, cascade (anti-cascade) efficiency is shown with circle (cross) symbol.

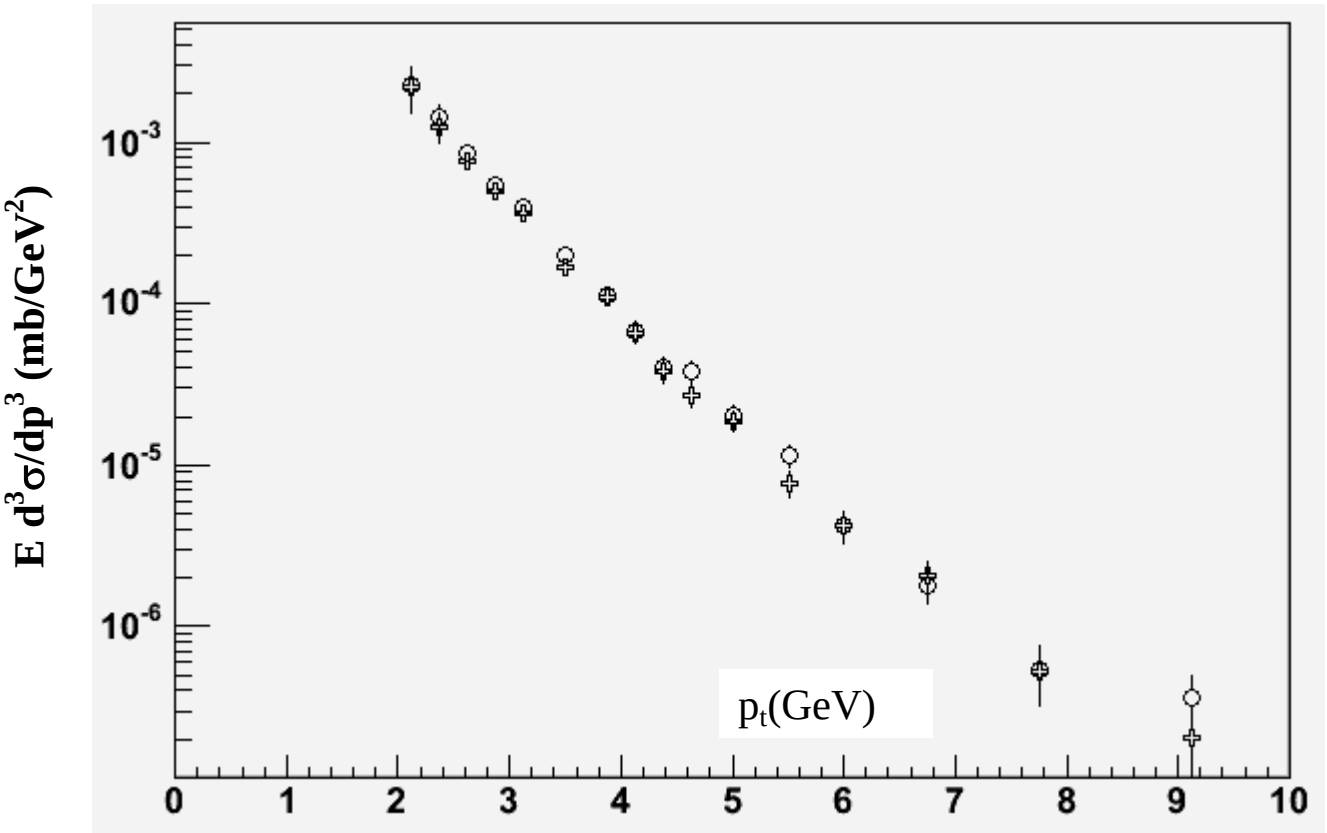

Figure 30. Cascade and anti-cascade invariant p_t cross section. Circle (cross) represents cascade (anti-cascade) data.

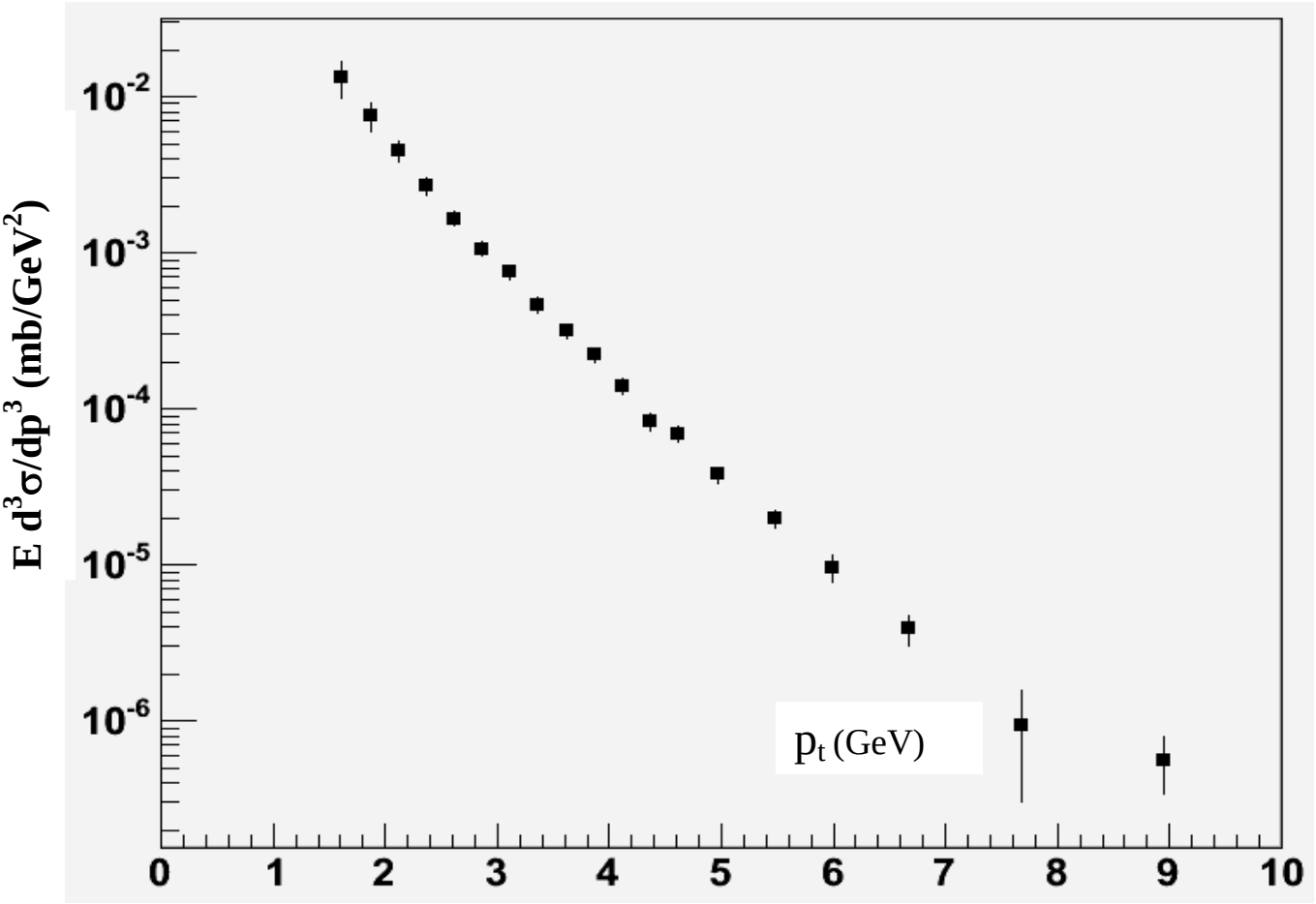

Figure 31. Cascade plus anti-cascade invariant p_t cross section.

The proper lifetime is calculated similar to Ks and lambdas. Figure 32 shows the lifetime for cascade candidates within the signal mass region (between 1.31 and 1.33 GeV) and within the sideband regions (1.295 and 1.305GeV, 1.335and 1.345 GeV) normalized to the background under cascade peak. Figure 33 is the sideband subtracted proper lifetime. The data is fitted with an exponential function and the lifetime of 3.5 +/- 0.1 cm is obtained. The same is carried out with MC data (Figure 34) and the lifetime is 3.6+/- 0.1 cm. Although the two values are consistent, this is lower than PDG's 4.9 cm. The difference is likely due to two reasons. One is the material effect. The material affects the lifetime in two ways: Cascades and lambdas interact with material before decaying. In addition the daughter particles interact with material such that they do not get reconstructed. The other reason is the 50 cm cut off. This tends to distort the decay distribution because the actual cut off is a function of p_t when the proper decay time is plotted.

The systematic error as a function of p_t is calculated similar to that of Ks except there are two more variations. The variations in Table 6 are used to evaluate the systematic errors. Figure 35 shows the ratio, R_i (p_t) of all variations and Figure 36 shows the systematic error.

	Default	Variation 1	Variation 2
p_t	.325 GeV	.300 GeV	.350 GeV
Z_1-Z_2	1.5 cm	1.0 cm	2.5 cm
decay length (L_Λ)	2.5 cm <L<50 cm	1.0 cm <L<50 cm	5.0 cm <L<50cm
$L_\Lambda - L_\Xi$	< 1.0 cm	3.0 cm	
d0 (Ξ)	0.25 cm	0.10 cm	-
δZ_0	2.0 cm	1.0 cm	5.0 cm
Number of Mix	four events	One event	-

Table 6. The variations used to calculate the cascade systematic errors

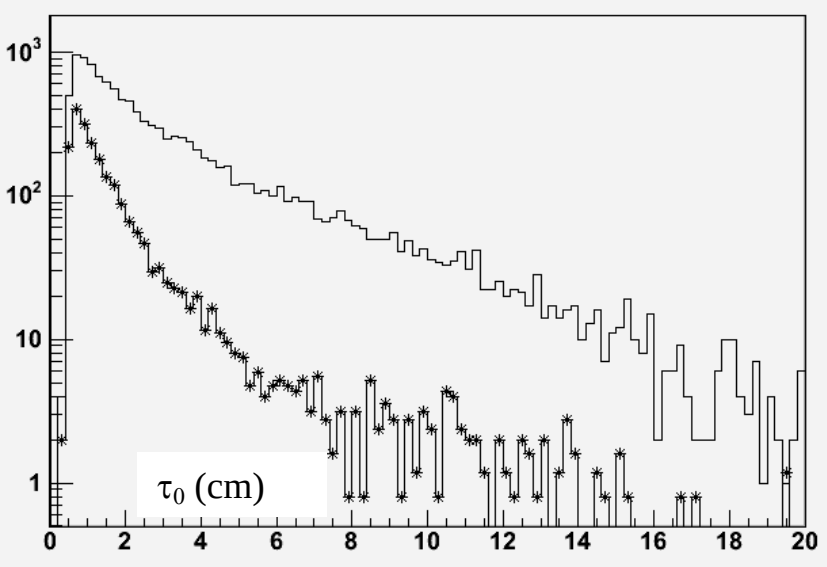

Figure 32. Proper lifetime of cascade candidates from the signal region and sideband regions(*).

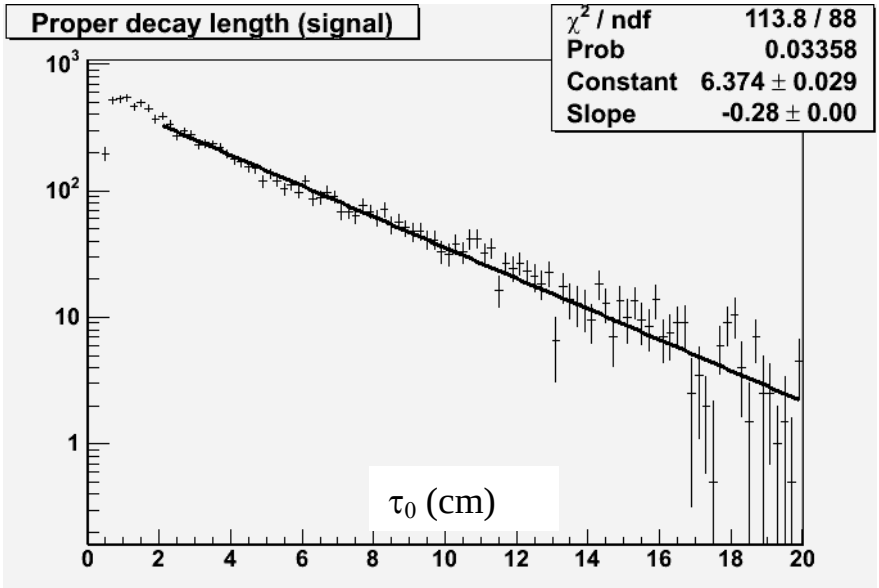

Figure 33. Proper lifetime of cascade after sideband subtraction.

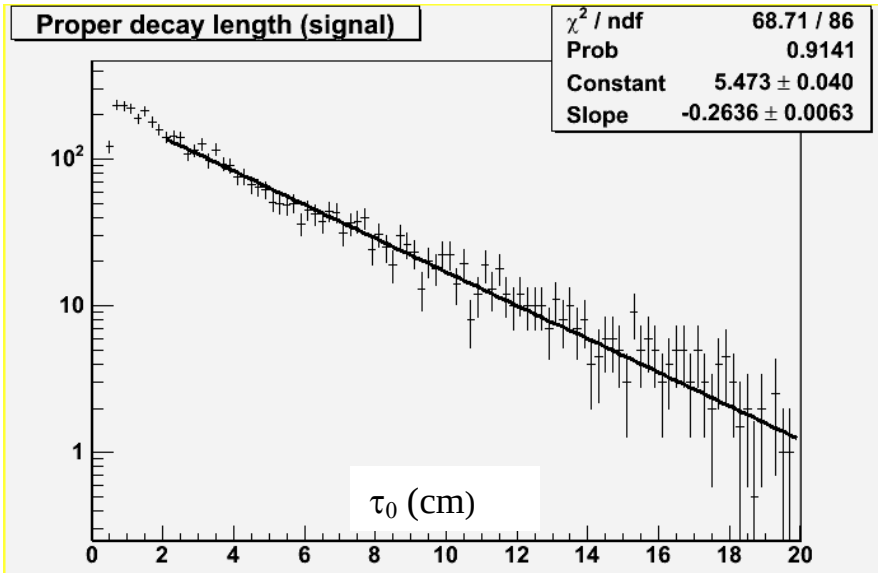

Figure 34. proper lifetime of cascades from MC data. 2 and 3GeV p_t cascades are used.

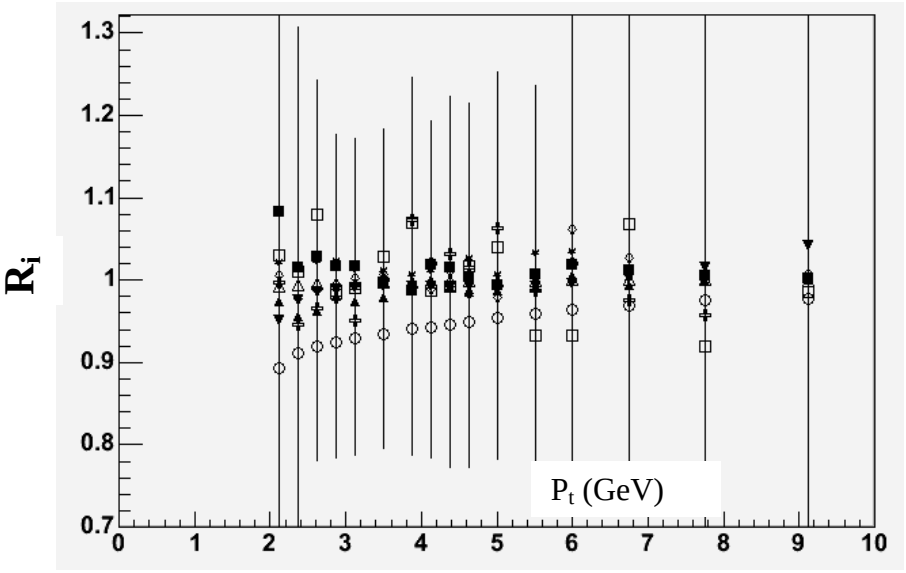

Filled square : pt> 0.35 GeV
Filled triangle : pt>0.30 GeV
Filled inverted triangle : 1 MB mixed
Open circle : |z1-z2| <2.5 cm
Open square : |z1-z2| <0.75 cm
Open triangle : L_Λ >1.0 cm
Open diamond : L_Λ > 5 cm
Cross : d_0 <0.10 cm
Filled star : δz_0 <5.0cm
Open star : L_Λ- L_Ξ <3.0 cm

Figure 35. R_i (p_t) distribution (ignore error bars).

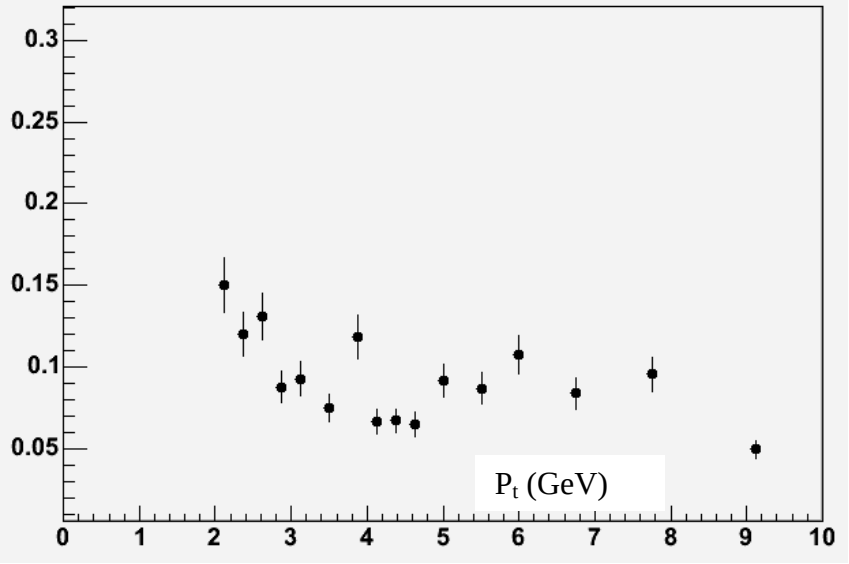

Figure 36. Cascade systematic error as a function of p_t.

9. Omega Reconstruction.

The omega reconstruction procedure is the same as the cascade reconstruction except the third track is assigned a kaon mass rather than a pion mass ($\Omega^- \rightarrow \Lambda K^- \rightarrow (p\pi^-)K^-$, $\Omega^+ \rightarrow \bar{\Lambda} K^+ \rightarrow (\bar{p}\pi^+)K^+$). Figure 37 show the invariant mass of the omega candidates for several p_t intervals after all cuts (Table 5). Unlike other resonances, the level of background is high. In order to calculate the number of omegas, before fitting the plots with a Gaussian plus a polynomial function, a background subtraction is made. The shape of the background is obtained using the lambda candidates outside the lambda mass cut, which are $1.095 < M_{p\pi} < 1.105$ GeV and $1.127 < M_{p\pi} < 1.137$ GeV. These candidates are processed like the candidates within the lambda mass cut. These background plots are shown with * symbol in Figure 37. The background is scaled to the number of events within the invariant mass 1.69 to 1.74 GeV. The scale factor is changed by a factor of 0.8 and its effect is put in as one of the systematic errors. The subtracted plot is fitted with a Gaussian plus a polynomial function (
Figure 38). After the fit, the polynomial background is subtracted and the number of omegas is obtained by counting the number of entries with mass between 1.65 and 1.67 GeV.

Figure 39 shows the omega and anti-omega efficiency as a function of p_t. Because of low statistics, we do not plot omega and anti-omega p_t spectra separately. Using the average efficiency of omegas and anti-omegas and the number of omegas previously calculated, the invariant p_t cross section is calculated and plotted in Figure 40. Also shown in the same figure is the spectrum obtained with 0.8 scale factor for the background subtraction in Figure 37. The difference is minor.

The systematic error as a function of p_t is similarly calculated as for cascades. The variations in Table 7 are also used to evaluate the systematic errors. There is one more variation which is the scale factor for the background subtraction. Figure 41 shows the ratio, R_i (p_t), of all variations and Figure 42 shows the combined systematic error. Although the combined systematic errors are expected to be similar to those for cascades, the errors are about a factor of two higher. This is due to the low statistics which affects the background subtracting and fitting. In other words, the R_i values have a large contribution from the background subtracting and fitting process. Since the uncertainty is counted every time a variation is tested, this contribution is counted multiple times when the final systematic error is calculated (Figure 42). Because of this effect, we used the cascade systematic errors (Figure 36) for omegas after including the effect of the background subtraction scale factor. This is reasonable since the only difference between the cascade and omega reconstruction is when the mass of the third track is assigned.

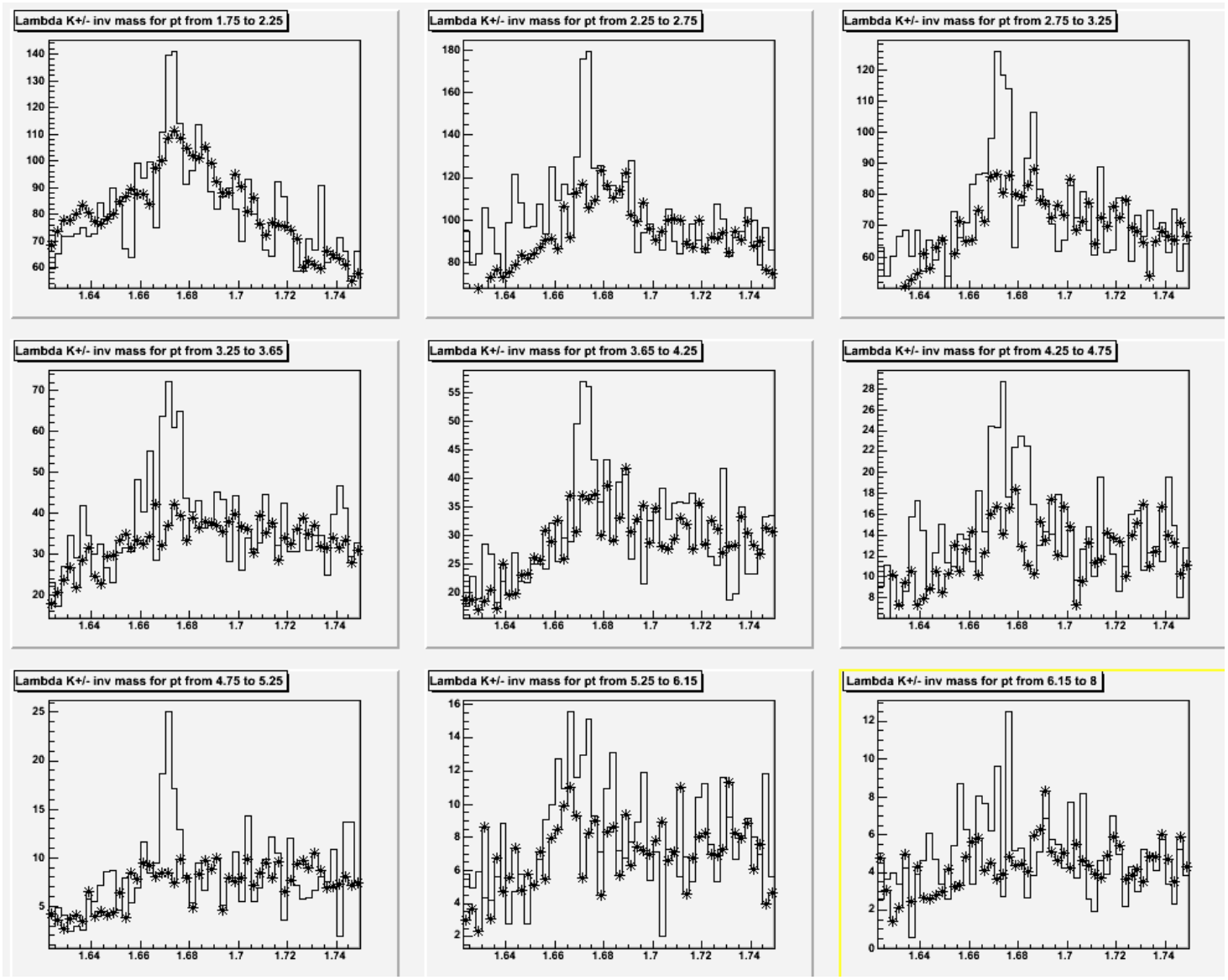

Figure 37. Invariant mass of omega plus anti-omega candidates. Histogram is from the signal region (within lambda mass window) and * is from sideband regions (outside the lambda mass window).

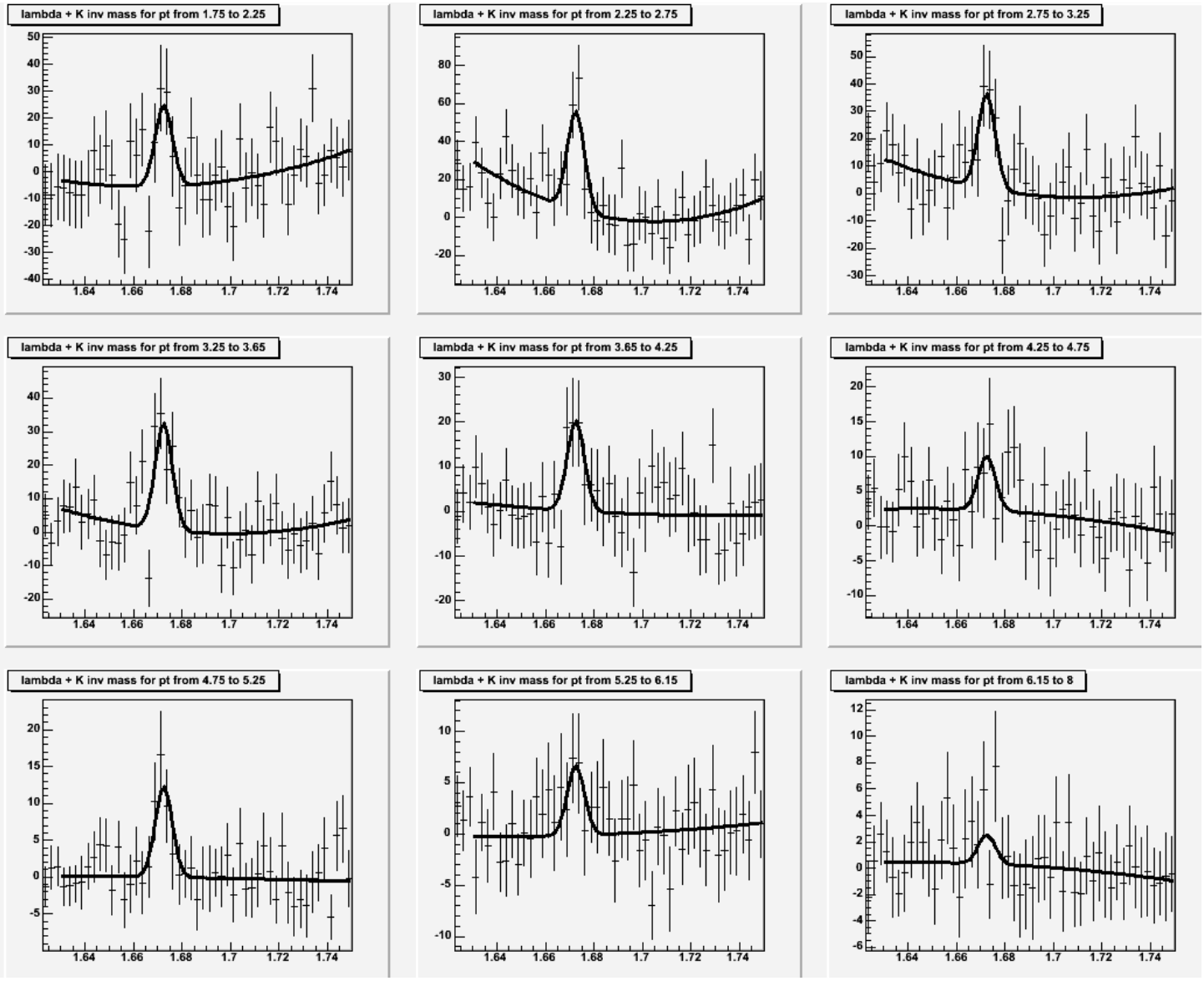

Figure 38. Invariant mass of omega plus anti-omega after the background is subtracted. For the fit, the sigma of the Gaussian is fixed at 0.003 GeV.

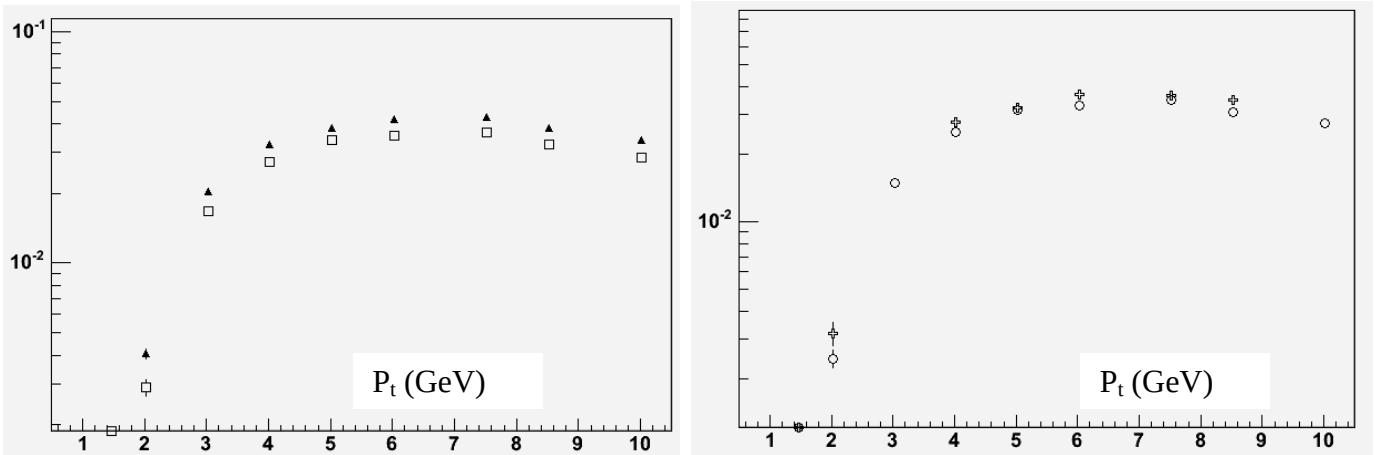

Figure 39. Omega reconstruction efficiency (triangle: one MB mixed, square: four MB mixed). In the right plot, the omega (anti-omega) efficiency points are shown with circle (cross) symbols.

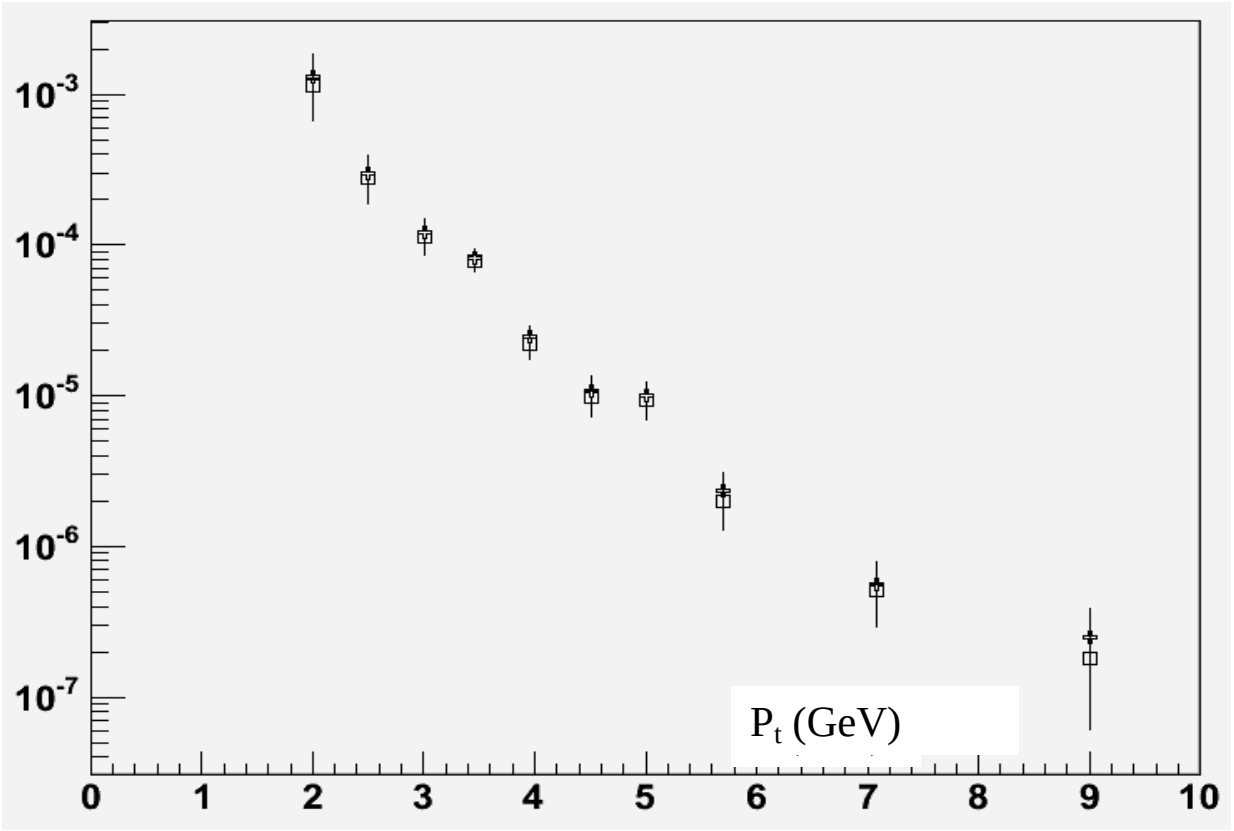

Figure 40. Omega invariant p_t cross sections. The points with cross symbol are with the background scale factor 0.8 (1.0 is the default).

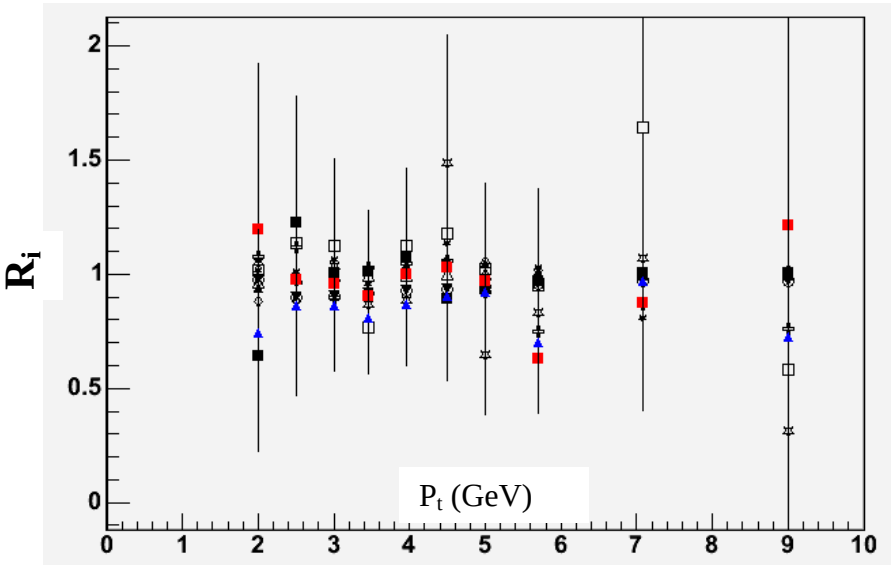

Filled square	: pt> 0.35 GeV
Filled triangle	: pt>0.30 GeV
Filled inverted triangle	: 1 MB mixed
Open circle	: |z1-z2| <2.5 cm
Open square	: |z1-z2| <0.75 cm
Open triangle	: L_Λ >1.0 cm
Open diamond	: L_Λ > 5 cm
Cross	: d_0 <0.10 cm
Filled star	: δz_0 <5.0cm
Open stat	: L_Λ- L_Ξ <3.0 cm
Red square	: Background scale: 0.6
Blue triangle	: Background scale: 0.8

Figure 41. R_i (p_t) distribution (ignore error bars).

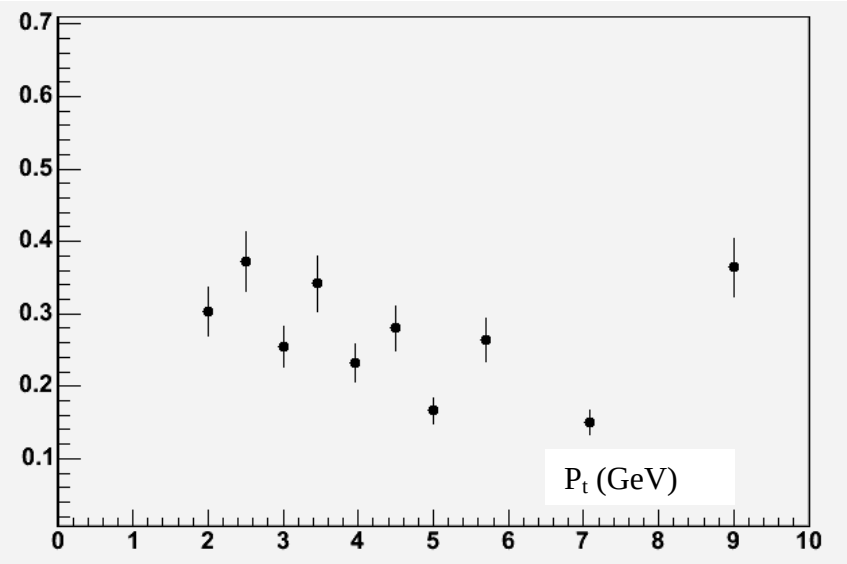

Figure 42. Omega systematic error as a function of p_t.

10. Invariant p_t cross section

Figure 43 shows the invariant p_t distribution for all hyperons with fitted power law curves, $(A)(p_0)^n /(p_t + p_0)^n$. Table 8 shows the fit results. To compare among different particles including Ks, p_0 is fixed at 1.3. A' is the amplitude at p_t = 2GeV. The curves are also fitted with an exponential function, and the fit results are in Table 9. The χ^2/dof are reasonable.

	Ks (Run I)	Lambda ($2<p_t<10$ GeV)	Cascade ($2<p_t<10$ GeV)	Omega ($2<p_t<10$ GeV)
A	51.6+/- 4.7	170+/-12	1.44+/-2.7	1.25+/-0.50
A'		$(4.9+/-0.13)\times10^{-2}$	$(7.0+/-0.4)\times10^{-3}$	$(7.9+/-1.3)\times10^{-4}$
N	7.79+/-0.06	8.70+/-0.04	8.20+/-0.14	7.9+/-0.35
P_0 (fixed)	1.3	1.3	1.3	1.3
χ^2/dof		22.1/15	16.8/15	10.9/8

Table 8. Results of fit to power function. A' is the amplitude at p_t=2GeV.

	Lambda ($1.2<p_t<2$GeV)	Lambda ($1.2<p_t<4$GeV)	Cascade ($1.5<p_t<4$ GeV)	Omega ($2.0<p_t<4$GeV)
B	4.9+/-1.0	3.33+/-0.20	0.156+/-0.043	0.019+/-0.009
B	2.30+/-0.13	2.10+/-0.02	1.73+/-0.10	1.75+/-0.15
χ^2/dof	3.5/4	18.7/12	3.0/8	6.5/3

Table 9. Results of fit to exponential function.

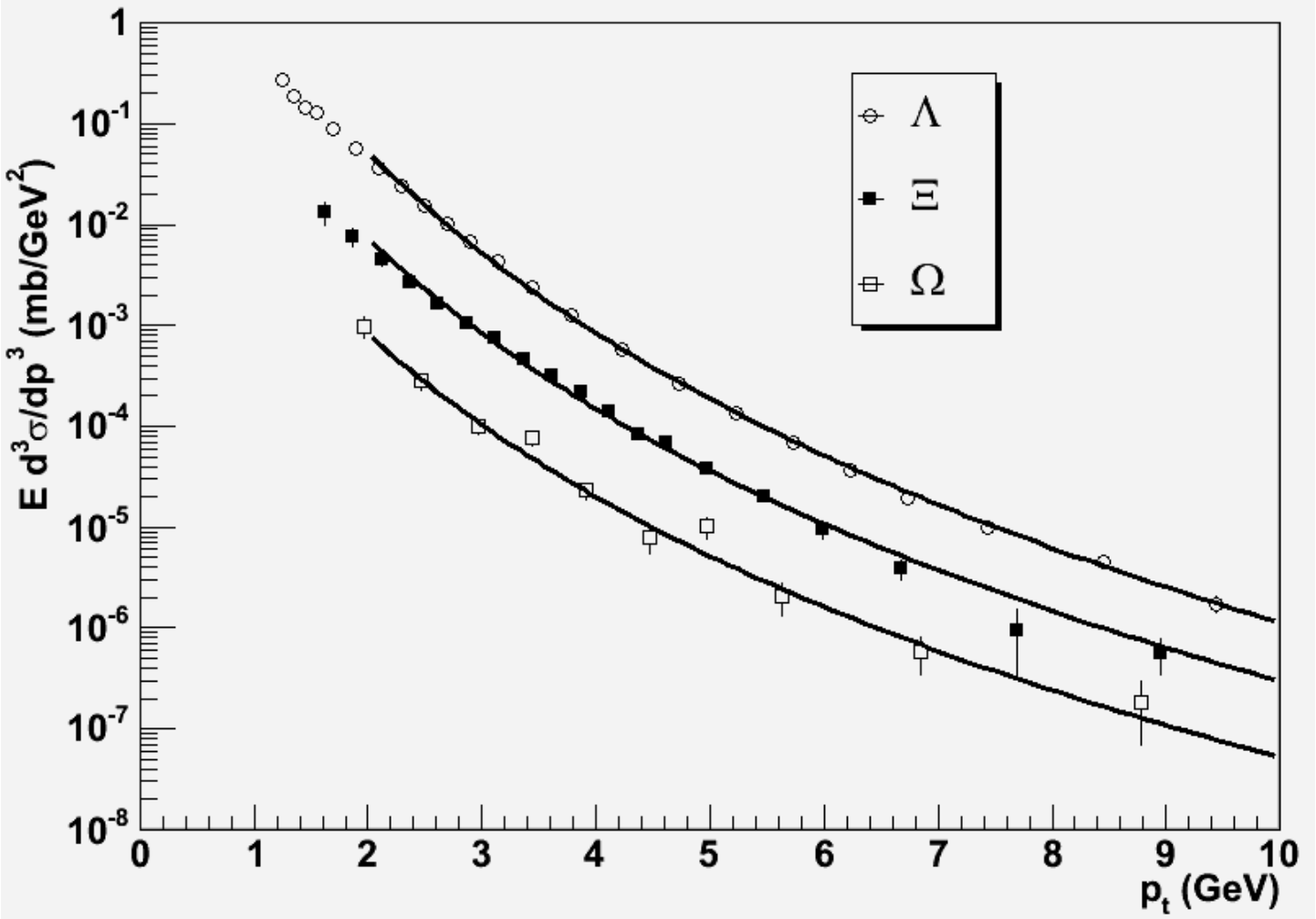

Figure 43. Invariant p_t cross section of lambda, cascade and omega (from the top to bottom). The curves are fits using the power law with fixed p_0.

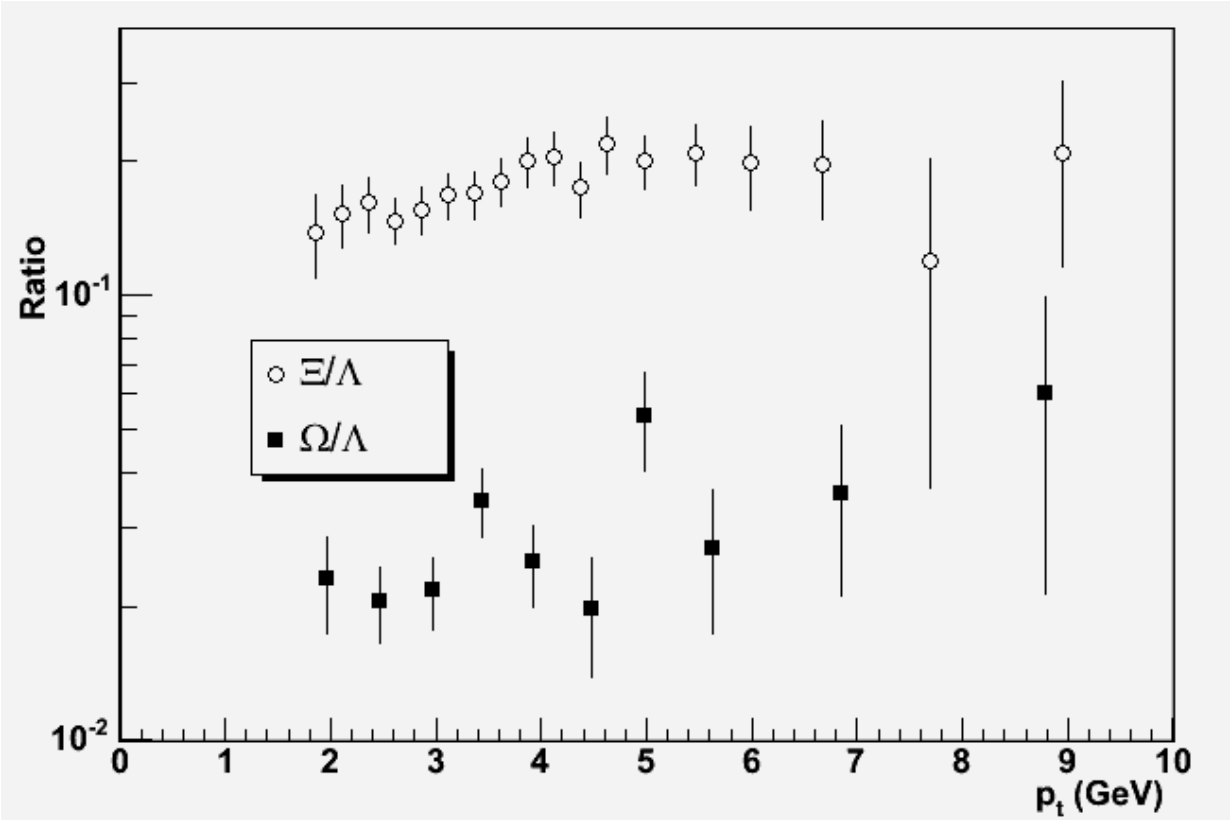

Figure 44. The ratio of cascade to lambda, and omega to lambda as a function of p_t.

Figure 44 shows the ratio of cascade to lambda and omega to lambda. For the cascade to lambda ratio, there is a gentle rise as p_t increases. If the ratio is fitted with a constant as a function of p_t, the ratio is 16.6+/- .6 %. For the omega to lambda ratio, the constant is 2.5+/-.3%. We should point out that not all lambdas are from the primary interaction. There are contributions from short lived resonances, such as $\Sigma^0 \rightarrow \Lambda\gamma$ ($\tau \sim 2\times10^{-11}$ cm). Another is from Ξ^- and $\Xi^0 \rightarrow \Lambda^0\pi^0$ ($\tau \sim 9$ cm) and their anti-particles. Some of them are removed by d0 and δz_0 vertex cuts, and a MC study shows that about ~50% of lambdas from Ξ^- and Ξ^0 pass the cuts.

Error! Reference source not found. shows the lambda invariant p_t cross section with multiplicity less than 10 and greater than 24. dn/dη (multiplicity density) for multiplicity 25 is about 16 including the tracks below p_t cut effect and track reconstruction efficiency above the p_t cutoff [7]. Figure 46 shows the ratio of the two plots in Figure 45. Before taking the ratio, the two plots are normalized at the beginning using the first two bins. Figure 47 shows the cascade invariant p_t cross section with multiplicity less than 10 and greater than 24 and Figure 48 shows the ratio of the two.

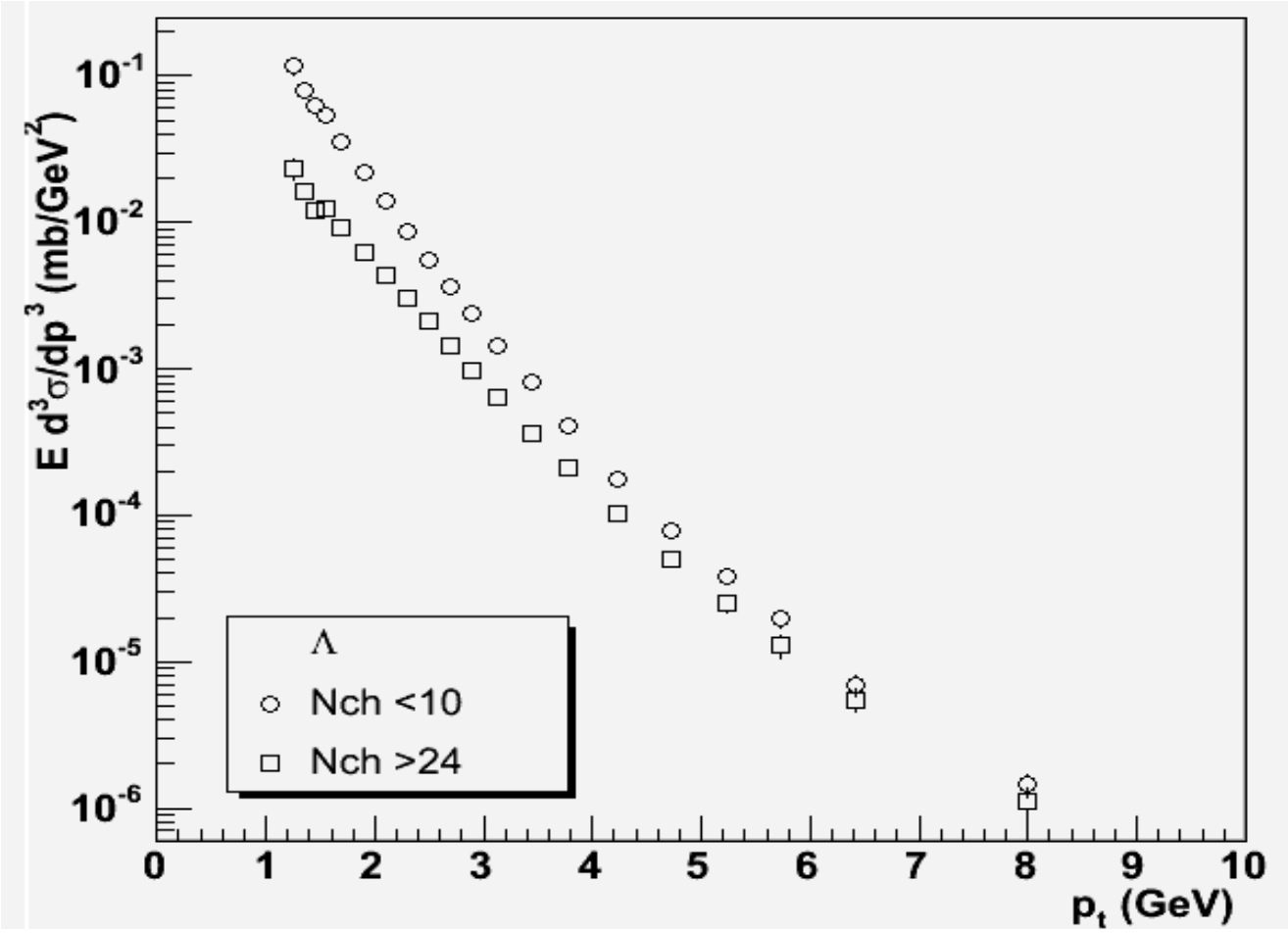

Figure 45. Lambda invariant p_t cross section with multiplicity less than 10 (circle symbols) and greater than 24 (square symbols).

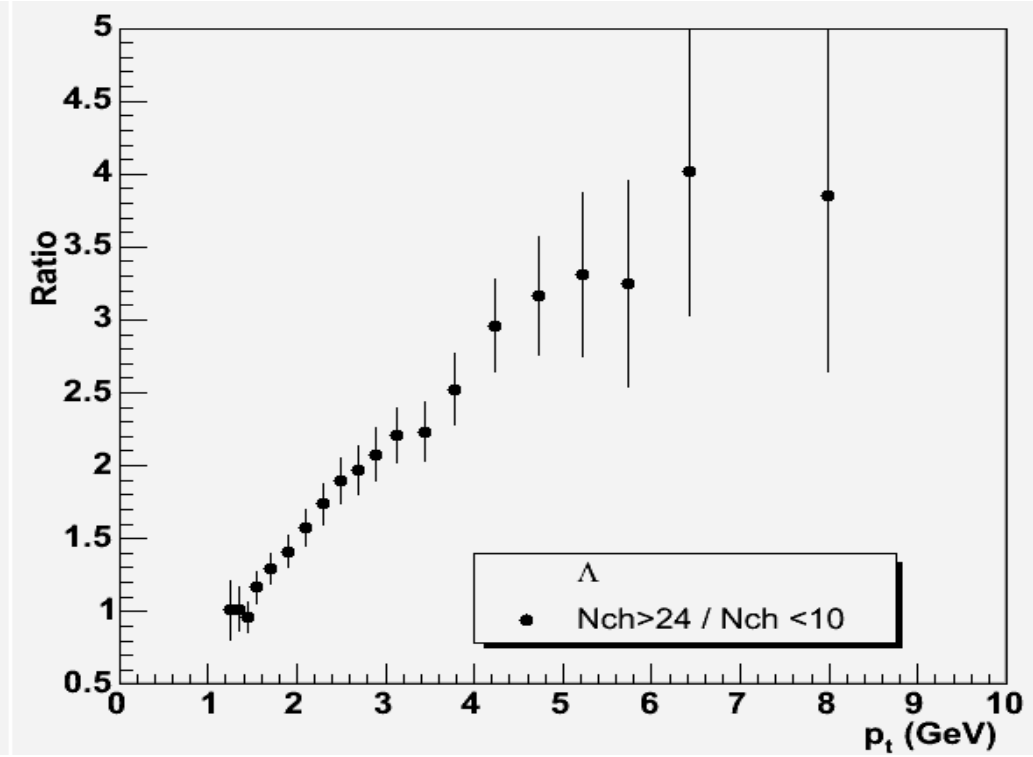

Figure 46. The ratio of the two plots in Figure 45. The two plots are normalized at the beginning using first two bins.

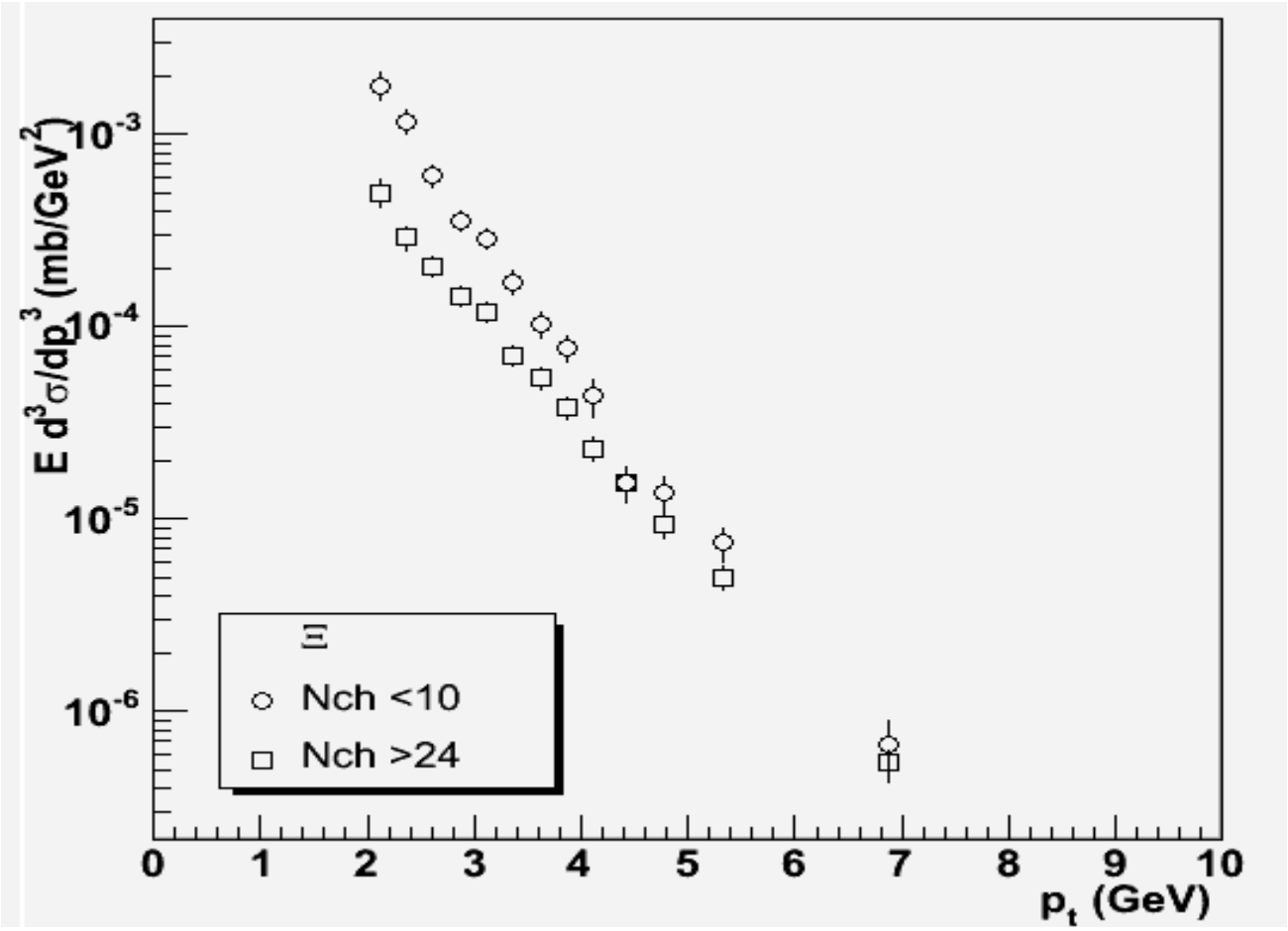

Figure 47. Cascade invariant p_t cross section with multiplicity less than 10 (circle symbols) and greater than 24 (square symbols).

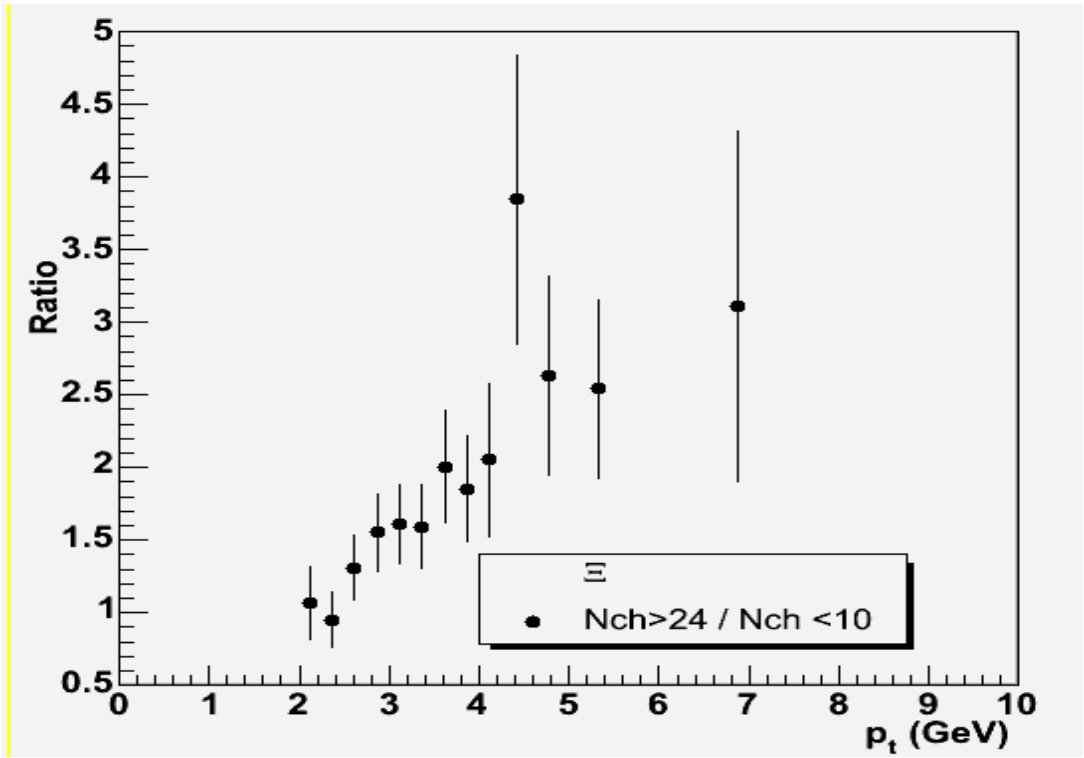

Figure 48. The ratio of the two plots in Figure 47. The two plots are normalized at the beginning using first two bins.

11. Summary

We have reported on the first extensive hyperon analyses based on ~100 million minimum biased events. Using the data, the inclusive invariant p_t distributions of lambdas, cascades and omegas and their production ratios as a function of p_t have been presented. The p_t distributions have been further divided into two multiplicity ranges.

12. References

[1]
[2] G. Alner et al., Phys. Lett. 151B, 309 (1985)
[3] S. Banerjee et al., Phys. Rev. Lett. 62, 12 (1989)
[4] T. Alexopoulos et al., Phys. Rev. D46, 2773 (1992)
[5] V. E. Barnes et al., Phys. Rev. Lett. 12, 204 (1964)
[6] F. Abe et al., Phys. Rev. D40, 3791 (1989)
[7] F. Abe et al., Phys. Rev. Lett. 61, 1819 (1988)